

Expectation Propagation in the large-data limit

Guillaume Dehaene, Simon Barthelmé

1st April 2016

Abstract

Expectation Propagation (Minka, 2001) is a widely successful algorithm for variational inference. EP is an iterative algorithm used to approximate complicated distributions, typically to find a Gaussian approximation of posterior distributions. In many applications of this type, EP performs extremely well. Surprisingly, despite its widespread use, there are very few theoretical guarantees on Gaussian EP, and it is quite poorly understood.

In order to analyze EP, we first introduce a variant of EP: averaged-EP (aEP), which operates on a smaller parameter space. We then consider aEP and EP in the limit of infinite data, where the overall contribution of each likelihood term is small and where posteriors are almost Gaussian. In this limit, we prove that the iterations of both aEP and EP are simple: they behave like iterations of Newton’s algorithm for finding the mode of a function. We use this limit behavior to prove that EP is asymptotically exact, and to obtain other insights into the dynamic behavior of EP: for example, that it may diverge under poor initialization exactly like Newton’s method. EP is a simple algorithm to state, but a difficult one to study. Our results should facilitate further research into the theoretical properties of this important method.

Introduction

Current practice in Bayesian statistics favors MCMC methods, but so-called *variational approximations* are gaining traction. In machine learning, where time constraints are primary, they have long been the favored method for Bayesian inference (Bishop, 2007). Variational methods provide fast, deterministic approximations to arbitrary distributions. Examples include mean-field methods (Wainwright and Jordan, 2008), INLA (Integrated Nested Laplace Approximation, Rue et al., 2009), and Expectation Propagation (EP).

EP was introduced in Minka (2001) and has proved to be one of the most durably popular methods in Bayesian machine learning. It gives excellent results in important applications like Gaussian process classification (Kuss and Rasmussen, 2005; Nickisch and Rasmussen, 2008) and is used in a wide range of applications (e.g., Jylänki et al. 2014, 2011; Gehre and Jin 2013; Ridgway et al. 2014). Recently EP has been shown to work very well in certain difficult likelihood-free settings (Barthelmé and Chopin, 2014), and has even been advocated as a generic form of inference in large-data problems (Gelman et al., 2014; Xu et al., 2014), since EP is easy to parallelize.

Most of the work on EP concerns applications, and focuses on making the method work well in various settings. Why and when the method should work remains somewhat of a mystery, and in this article we aim to make progress in that direction. A few theoretical results are available when the approximating family is a discrete distribution, in which case EP is equivalent to Belief Propagation, a well-studied algorithm (Wainwright and Jordan, 2008). The typical case in Bayesian inference is to use multivariate Gaussians as the approximating family, but very little is known about that case: Ribeiro and Opper (2011) study a limit of EP for neural network models (the limit of infinitely many weights) and Titterton (2011) gives partial results on mixture models in the large-data limit. Despite these efforts, two aspects of EP’s behavior have remained elusive: its dynamical behavior (does the EP iteration converge on a *fixed dataset*?) and its large-data behavior (do fixed points of the iteration converge to the target distribution in the limit of infinite data?). In this work, we focus on the dynamical behavior of EP and show that it is asymptotically equivalent to the behavior of Newton’s method (Nocedal and Wright, 2006). This enables us to prove that EP is exact in the large-data limit: if the posterior in the large-data limit tends to a Gaussian (as they usually do), then EP recovers the limiting Gaussian. Furthermore, we show that on multimodal distributions, EP often has one fixed-point for each mode. This also yields insights into why EP iterations can be so unstable.

The outline of the paper is as follows. In section 1, we give a quick introduction to EP and introduce a simpler variant which we call averaged-EP (aEP). aEP is mathematically simpler than EP because it iterates over a much smaller parameter space (independent of n , the number of data points), which makes our results easier to state and to understand. We then

present our theoretical contributions in section 2. Our main result concerns the asymptotic behavior of the EP update, which turns out to be extremely simple. This asymptotic behavior has many consequences, of which we highlight two. First, EP and aEP asymptote to Newton’s algorithm. Second, EP is asymptotically exact, or more specifically the target distribution and one specific EP fixed-point converge in total-variation distance. In section 3, we then show that this Newton limit behavior of EP can give us some intuition into how the iterations of the algorithm work. Finally, in section 4 we discuss limitations of our results and give directions for future work.

Notation and background

Vectors are in bold, matrices are in bold and capitalized. Given a multivariate function $f(\mathbf{x})$, we note ∇f its gradient and Hf its Hessian, the matrix of the second derivatives. Univariate Gaussian distributions are represented as $\mathcal{N}(x|\mu, v) \propto \exp\left(-\frac{1}{2v}(x - \mu)^2\right)$, although occasionally the exponential parameters $\beta = v^{-1}$, $r = \beta\mu$ are used: $\mathcal{N}(x|r, \beta) \propto \exp\left(-\frac{1}{2}\beta x^2 + rx\right)$. We call β the *precision* and r the *linear shift*. Table 1 provides a lexicon for EP and a summary of the notation.

The goal of EP is to compute a Gaussian approximation of a target distribution, which we note $p(\mathbf{x}) \propto \exp(-\psi(\mathbf{x}))$. This distribution factorizes into n factor-functions (sites in EP terminology): $p(\mathbf{x}) = \prod_{i=1}^n l_i(\mathbf{x})$. We note $\phi_i(\mathbf{x}) = -\log(l_i(\mathbf{x}))$. EP produces a Gaussian approximation $q(\mathbf{x}) \approx p(\mathbf{x})$ with the same factor structure, n Gaussian factors $f_i(\mathbf{x})$ such that: $q(\mathbf{x}) = \prod_{i=1}^n f_i(\mathbf{x})$. Each Gaussian factor $f_i(\mathbf{x})$ approximates the corresponding target factor $l_i(\mathbf{x})$.

Newton’s algorithm as an approximate inference method

Approximate inference methods aim to find a tractable approximation $q(\mathbf{x})$ to a complicated density $p(\mathbf{x})$. Most of them operate by solving:

$$\operatorname{argmin}_{q \in \mathcal{Q}} D(p||q)$$

where \mathcal{Q} denotes some set of tractable distributions and D is a divergence measure. Depending on the choice of divergence measure and approximating distribution, one can derive various variational algorithms. These methods are often iterative and produce a sequence of approximations q_1, \dots, q_T that should hopefully tend to a locally optimal approximation.

One of our key results proves that, in the large-data limit (denoted here by $n \rightarrow \infty$), EP behaves like Newton’s algorithm (NT, see e.g. Nocedal and Wright, 2006 for an introduction). NT aims to find a mode of a target probability distribution $p(x) \propto \exp(-\psi(x))$ through an iterative procedure. We present here the one-dimensional version. Once initialized at a point μ_1 , a sequence of points (μ_t) is constructed with:

$$\mu_{t+1} = \mu_t - \left[\psi''(\mu_t)\right]^{-1} \psi'(\mu_t) \tag{1}$$

This iteration can be viewed as a gradient descent with a Hessian correction. It can also be viewed as approximating $\log(p)$ as its second degree Taylor expansion around μ_t , and then setting μ_{t+1} as the extremum of that polynomial.

With a slight modification we can restate NT as an approximate inference algorithm iterating on Gaussian approximations of p , which makes the parallel to EP more obvious. Starting from an arbitrary Gaussian g_1 , with mean μ_1 , we construct a sequence of Gaussian approximations (g_t) through iterating the following steps:

1. Compute $\delta r_{t+1} = -\psi'(\mu_t)$ and $\beta_{t+1} = \psi''(\mu_t)$
2. Compute a Gaussian approximation to $p(x)$: $g_{t+1}(x) \propto \exp\left(\delta r_{t+1}(x - \mu_t) - \beta_{t+1} \frac{(x - \mu_t)^2}{2}\right)$
3. Compute the mean of g_{t+1} : $\mu_{t+1} = \mu_t - \left[\psi''(\mu_t)\right]^{-1} \psi'(\mu_t)$

With this change, the fixed point of NT is now the Gaussian distribution $\mathcal{N}\left(x \middle| x^*, \left[\psi''(x^*)\right]^{-1}\right)$ centered at x^* , the mode of p , and with precision the Hessian of $\log(p)$ at the mode x^* . Thus, the fixed point of this NT variant is the canonical Gaussian approximation (CGA) at the mode of p , also sometimes referred to as the “Laplace” approximation (which is erroneous as the Laplace approximation actually refers to approximating integrals and not probability distributions).

Term	Explanation
Target distribution	The distribution we wish to approximate: $p(\mathbf{x}) \propto \prod_{i=1}^n l_i(\mathbf{x})$
EP approximation	An exponential-family distribution with the same factor structure as $p(\mathbf{x})$, $q(\mathbf{x}) \propto \prod_{i=1}^n f_i(\mathbf{x}) = \frac{\exp(\sum \lambda_i^t \mathbf{s}(\mathbf{x}))}{Z(\sum \lambda_i)}$
“Site” or “factor”	A factor $l_i(\mathbf{x})$ in the target distribution
Site approximation	A factor $f_i(\mathbf{x})$ in the approximation
Cavity prior	The approximate distribution with site i taken out, i.e. $q_{-i}(\mathbf{x}) \propto \exp\left(\sum_{j \neq i} \lambda_j^t \mathbf{s}(\mathbf{x})\right)$. In aEP, $q_{-i}(\mathbf{x}) \propto q_{-i}^{\frac{n-1}{n}}(\mathbf{x})$ is independent of i .
Hybrid distribution	The product of a cavity prior and a true site, i.e.. $h_i(\mathbf{x}) \propto q_{-i}(\mathbf{x}) l_i(\mathbf{x})$

Table 1: An EP lexicon

An important issue is the convergence of NT. It has fast convergence when initialized close to a mode of p . Technically, convergence is quadratic, i.e. $|\mu_{t+1} - x^*| \leq c(\mu_t - x^*)^2$. However, that is only true in a neighborhood of the mode and the basic version of the algorithm, which we presented here, does not generally converge for all starting points μ_1 . In order to obtain an algorithm with guaranteed convergence, one solution is to complement NT with a line-search algorithm. As we shall see, EP can also have unstable behavior when initialized too far from its fixed points: we return to this important issue in section 3.1.

Log-concave distributions and the Brascamp-Lieb theorem

Our theoretical results depend on a very powerful theorem on log-concave probability distributions, called the Brascamp-Lieb theorem (Brascamp and Lieb, 1976; Saumard and Wellner, 2014). Let $LC(\mathbf{x}) \propto \exp(-\psi(\mathbf{x}))$ be a log-concave distribution (i.e., $H\psi(\mathbf{x})$ is always symmetric positive definite). The variance of any statistic $S(\mathbf{x})$ is then bounded according to:

$$\text{var}_{LC}(S(\mathbf{x})) \leq E_{LC} \left((\nabla S)^T [H\psi(\mathbf{x})]^{-1} \nabla S \right) \quad (2)$$

We use this result in the particular case $S(\mathbf{x}) = \mathbf{x}$ from which we get an upper-bound on the variance:

$$\text{var}_{LC}(\mathbf{x}) \leq E_{LC} \left([H\psi(\mathbf{x})]^{-1} \right) \quad (3)$$

Further more, if the log-Hessian is lower-bounded (as a matrix inequality): $H\psi(\mathbf{x}) \geq \mathbf{B}_m$, then the variance has an even simpler upper-bound:

$$\text{var}_{LC}(\mathbf{x}) \leq \mathbf{B}_m^{-1} \quad (4)$$

1 From classic EP to averaged-EP (aEP)

Classic EP

In this section we introduce EP in the exponential-family notation used by Seeger (2005), because it is neat, generic and compact. EP has been introduced from a variety of viewpoints, and the versions given in Minka (2005); Seeger (2005); Bishop (2007); Raymond et al. (2014) are all potentially useful.

Following Minka (2005), given a target distribution $p(\mathbf{x})$, EP aims to solve

$$\underset{q \in \mathcal{Q}}{\text{argmin}} KL(p||q) \quad (5)$$

where \mathcal{Q} is an approximating family and KL denotes the Kullback-Leibler divergence. Here we focus on the Gaussian case but other exponential families may be used (for example, the Gaussian-Wishart family is used in Paquet et al., 2009).

A central aspect of EP is that it relies on a *factorization* of p , i.e. that the posterior decomposes into a product of terms:

$$p(\mathbf{x}) = \frac{1}{Z} \prod_{i=1}^n l_i(\mathbf{x}) \quad (6)$$

where usually one of the terms corresponds to the prior and the rest to independent likelihood terms (here and elsewhere $Z = \int \prod_{i=1}^n l_i(\mathbf{x}) d\mathbf{x}$ is a normalization constant). The decomposition is non-unique and the performance and feasibility of EP depend on the factorization one picks. The approximation has the same factor structure:

$$q(\mathbf{x}) \propto \prod_{i=1}^n f_i(\mathbf{x}) \quad (7)$$

Following Seeger, we call the l_i 's *sites* and the corresponding f_i 's *site approximations*. The site approximations have exponential-family form (e.g., Gaussian)

$$f_i(\mathbf{x}) = \exp(\boldsymbol{\lambda}_i^t \mathbf{t}(\mathbf{x}))$$

which the approximation inherits

$$q_{\boldsymbol{\lambda}_s}(\mathbf{x}) = \exp\{\boldsymbol{\lambda}_s^t \mathbf{t}(\mathbf{x}) - \phi(\boldsymbol{\lambda}_s)\} \quad (8)$$

where $\boldsymbol{\lambda}_s = \sum \boldsymbol{\lambda}_i$. Note that $\boldsymbol{\lambda}_s$ represents the so-called natural parameters for the approximation. According to a well-known property of exponential families, the gradient of the partition function, $\nabla \phi(\boldsymbol{\lambda})$ returns the expected value of the sufficient statistics for a given value of the natural parameters:

$$\boldsymbol{\eta} = \nabla \phi(\boldsymbol{\lambda}) = \frac{1}{Z} \int \mathbf{t}(\mathbf{x}) \exp\{\boldsymbol{\lambda}^t \mathbf{t}(\mathbf{x})\} d\mathbf{x}$$

Its inverse $\nabla \phi^{-1}$ transforms expected values of the sufficient statistics into natural parameters.

A well known result for exponential families shows that the global solution of problem (5) is a moment-matching solution:

$$\boldsymbol{\eta}^* = E_p(\mathbf{t}(\mathbf{x}))$$

In the Gaussian case, what this means is that the best approximation of p according to KL divergence is a Gaussian with the same mean and covariance. Of course, directly computing the mean and covariance of p is intractable, and so EP tries to get there by successive refinements of an approximation.

Specifically, EP tries to improve the approximation sequentially by introducing *hybrid* distributions which interpolate between the current approximation and the true posterior. A hybrid distribution h_i contains one site from the *true posterior*, but all the rest come from the approximation:

$$h_i(\mathbf{x}) \propto q_{-i}(\mathbf{x}) l_i(\mathbf{x}), \quad q_{-i}(\mathbf{x}) = \prod_{j \neq i} f_j(\mathbf{x}). \quad (9)$$

Hybrids should be tractable, meaning that one should be able to compute their moments quickly. Note that in exponential-family notation, the $q_{-i}(\mathbf{x})$ distribution is simply:

$$q_{-i}(\mathbf{x}) \propto \exp\{(\boldsymbol{\lambda}_s - \boldsymbol{\lambda}_i)^t \mathbf{t}(\mathbf{x})\}$$

EP improves the approximation sequentially by (a) picking a site i (b) computing the moments of the hybrid h_i and (c) setting $\boldsymbol{\lambda}_s$ such that the moments of $q_{\boldsymbol{\lambda}_s}$ match the moments of the hybrid.

Classic EP (Alg. 1) loops over the sites sequentially.

A parallel variant forms all the hybrids at once, looping several times over the whole dataset (Alg. 2).

Algorithm 1 Classic EP in exponential family form

Loop until convergence

For i in $1 \dots n$

1. Compute “cavity” parameter $\lambda_{-i} \leftarrow \lambda_s - \lambda_i$
2. Form hybrid distribution and compute its moments

$$\eta_i = \frac{1}{Z_i} \int \mathbf{t}(\mathbf{x}) l_i(\mathbf{x}) \exp \{ \lambda_{-i}^t \mathbf{t}(\mathbf{x}) - \phi(\lambda_{-i}) \} d\mathbf{x}$$

3. Update global parameter $\lambda_s \leftarrow \nabla \phi^{-1}(\eta_i)$, site parameter $\lambda_i \leftarrow \lambda_s - \sum_{j \neq i} \lambda_j$
-

Algorithm 2 Parallel EP

Loop until convergence

1. Process all hybrids: for i in $1 \dots n$
 - (a) Compute “cavity” parameters $\lambda_{-i} \leftarrow \lambda_s - \lambda_i$
 - (b) Form hybrid distribution and compute moments

$$\eta_i = \frac{1}{Z_i} \int \mathbf{t}(\mathbf{x}) l_i(\mathbf{x}) \exp \{ \lambda_{-i}^t \mathbf{t}(\mathbf{x}) - \phi(\lambda_{-i}) \} d\mathbf{x}$$

- (c) Compute local update $\lambda_i \leftarrow \nabla \phi^{-1}(\eta_i) - \sum_{j \neq i} \lambda_j$
 2. Update global parameters $\lambda_s \leftarrow \sum \lambda_i$
-

Averaged EP

We introduce a simpler variant of EP with a drastically reduced parameter set: namely, we get rid of all site-specific parameters λ_i and keep only global parameters λ_s . The resulting algorithm is simpler to analyze. Our variant is straightforward, and follows from setting $\lambda_i = \frac{1}{n} \lambda_s$ for all i , under the assumption that the contributions from all sites are be similar.

Proceeding step-by-step from alg. 2 we begin with the cavity parameter, which becomes $\lambda_c = \lambda_s - \frac{1}{n} \lambda_s = \frac{n-1}{n} \lambda_s$ independent of i . We use the cavity parameter to form hybrid distributions just as before:

$$h_i(\mathbf{x}) \propto l_i(\mathbf{x}) \exp \left\{ \frac{n-1}{n} \lambda_s^t \mathbf{t}(\mathbf{x}) \right\}$$

The moments of the hybrids are again noted η_i , and inserting the local updates into the update for the global parameter we get (recall that $\nabla \phi^{-1}$ transforms moment parameters into natural parameters):

$$\begin{aligned} \lambda'_s &= \sum \{ \nabla \phi^{-1}(\eta_i) - \lambda_c \} = \sum \left\{ \nabla \phi^{-1}(\eta_i) - \frac{n-1}{n} \lambda_s \right\} \\ &= \sum \nabla \phi^{-1}(\eta_i) - (n-1) \lambda_s \end{aligned} \tag{10}$$

It is interesting to examine the fixed points of this update rule, which satisfy:

$$\lambda_s^* = \sum \nabla \phi^{-1}(\eta_i | \lambda_s^*) - (n-1) \lambda_s^*$$

or equivalently:

Algorithm 3 averaged-EP

Loop until convergence

1. Compute “cavity” parameters $\lambda_c \leftarrow \frac{n-1}{n} \lambda_s$
2. For i in $1 \dots n$, form hybrid distribution and compute moments

$$\eta_i \leftarrow \frac{1}{Z_i} \int \mathbf{t}(\mathbf{x}) l_i(\mathbf{x}) \exp \{ \lambda_c^t \mathbf{t}(\mathbf{x}) - \phi(\lambda_c) \} d\mathbf{x}$$

3. Update global parameters $\lambda'_s \leftarrow \sum \nabla \phi^{-1}(\eta_i) - (n-1) \lambda_s$
-

$$\lambda_s^* = \frac{1}{n} \sum \nabla \phi^{-1}(\eta_i | \lambda_s^*)$$

where the hybrid moments η_i depend implicitly on λ_s . The following averaging rule shares the same fixed points:

$$\lambda'_s = \frac{1}{n} \sum \nabla \phi^{-1}(\eta_i | \lambda_s) \tag{11}$$

and that is the rule that gives averaged-EP (aEP) its name¹.

The resulting method is given in Alg. 3 but can be summarized in a few words. To improve an exponential-family approximation aEP begins by forming n hybrids of the approximation and the true posterior, it computes their moments, uses those to compute the new site approximations and the corresponding natural parameters, and sets the new natural parameters of the approximation to the sum of the site approximations.

2 Asymptotic behavior of the EP and aEP updates

In this section, we investigate the dynamics of the EP and aEP algorithms. We first present a new key result on the asymptotic behavior of the EP approximation of a site: we show that as the variance of the cavity q_{-i} converges to 0, the approximation converges to a simple Taylor approximation of $\log(l_i)$. This asymptotic behavior has several consequences but we present here the most important one: in the limit where all cavity priors q_{-i} have small variance, the parallel EP and the aEP updates converge towards the updates of Newton’s algorithm. A corollary is that, for multimodal target distributions, all modes which have sufficient curvature have an associated EP fixed point and that, as a certain measure of mode peakedness goes to infinity, the EP fixed point converges to the CGA at that mode. Finally, this enables us to prove that EP is asymptotically exact in the large-data limit (if the CGA also is).

2.1 Assumptions

Throughout this section, we work in the one-dimensional case since it is the easiest to understand. All results are straightforward to extend to the p -dimensional case (i.e., when the target distribution is p -dimensional), the most significant difficulty being notation. In the appendix, we give the proofs for the p -dimensional case.

We use two assumptions on the sites $l_i(x)$.

Both our conditions concern the negative log-likelihood of the sites $\phi_i(x) = -\log(l_i(x))$. Our first assumption is that the second log-derivative of the sites has a bounded range: there exists B such that:

$$\forall i, x \quad \max \left(\phi_i''(x) \right) - \min \left(\phi_i''(x) \right) \leq B \tag{12}$$

Our second condition concerns bounding some higher log-derivatives of the sites, which ensures that all sites are sufficiently regular so that we can use Taylor expansions and bound the remainder terms. Our assumption is simply that there exist bounds K_3 and K_4 which bound the third and fourth derivatives of all ϕ_i functions. For $d \in \{3, 4\}$:

$$\forall i, x \quad \left| \phi_i^{(d)}(x) \right| \leq K_d \tag{13}$$

¹Note that it corresponds to a slowed down version of the aEP update

Both of those conditions are easy to check in practice. For example, for a Generalized Linear Model, we would simply need to check the derivatives of the link function and that the design matrix is bounded and of full column rank. The one important case for which we cannot apply our result concerns non-parametric models, and, more generally, cases in which p is not fixed but grows. This reflects a limitation of our proof, rather than one of EP, which works just fine in such cases (see Appendix for details).

An important thing to note is that we chose those two assumptions because they give very simple expressions for the error of the asymptotic expression, but the limit behavior we present can still be reached even if they are broken. In the appendix, we show how weaker assumptions (bounded $l_i(x)$ and local smoothness of $\phi_i(x)$) are sufficient to obtain our results on the limit behavior with similar asymptotic errors.

2.2 Limit behavior of the EP update

2.2.1 Limit behavior of the site update

The only complicated step in EP and aEP (especially in practical implementation) is the site-approximation update during which we form the hybrid distribution, compute its moments and then subtract the contribution of the cavity to obtain the approximation of the site. We study here the limit behavior of the site-approximation as the cavity becomes more and more precise. The result we obtain is essential to the rest of this work, but not entirely intuitive, so our explanation will be progressive and careful.

What we are interested in is the limit behavior of the site update, as the precision of the cavity becomes large. The reason we focus on the high-precision limit is that, when there are many sites (datapoints), each individual one makes a small contribution compared to the rest. The cavity represents the contribution of all the other sites, and generally speaking the more sites there are the lower the variance of the cavity (the higher the precision). In large-data settings, the cavity prior tends to dominate the site’s likelihood, meaning that at the level of individual sites, *the “large data” limit becomes a “weak data” limit.*

To study that limit, our first object of interest is naturally the hybrid:

$$h_i(x) \propto l_i(x) \exp\left(-\frac{\beta}{2}x^2 + (\beta\mu_0)x\right)$$

where we have parametrized the cavity precision as β , and the cavity mean stays constant (at μ_0 throughout)². As β grows large, the cavity prior (the Gaussian part) outweighs the likelihood, and the hybrid starts to resemble a Gaussian centered at μ_0 with variance β^{-1} . Indeed those are provably the limits of the mean and variance of h_i when $\beta \rightarrow \infty$.

When β is large, the hybrid is almost the same as the cavity, and it is tempting to conclude that when β is large no update happens (the cavity prior outweighs the likelihood l_i , the site becomes negligible). That line of reasoning, although tempting, is misleading, as an examination of the case of a Gaussian site shows. Suppose

$$l_i(x) = \exp\left(-\frac{\gamma}{2}x^2 + \alpha x\right)$$

then, regardless of how large β is, it is straightforward to show that the site’s natural parameters are always $\beta_i = \gamma$ and $r_i = \alpha$. In other words: even when the prior outweighs the likelihood, the site always increases the overall precision by an additive factor and contributes to the overall linear shift.

In the non-Gaussian case the site’s natural parameters also have a non-trivial limit. The exact form of that limit turns out to be very interesting, as it shares a close relationship to Newton’s method. Specifically, we show that r_i reflects the gradient of the log-likelihood at the cavity mean and β_i the Hessian. In other words, the log of the site-approximation tends towards the Taylor expansion around μ_0 of the log-site $\phi_i(x)$. Fig. 1 illustrates that behavior in a simple scenario, where:

$$h_i(x) = \left(\frac{1}{1+e^{-x}}\right) \exp\left(-\frac{\beta}{2}x^2\right) \tag{14}$$

which corresponds to a logit likelihood and a cavity prior centered at 0. Here $\phi_i = \log(1+e^{-x})$, $\phi_i'(0) = -\frac{1}{2}$, and $\phi_i''(0) = \frac{1}{4}$.

²In the notation of the previous section, the natural parameters are $\lambda = [\beta \quad \beta\mu_0]^t$, the precision and linear shift.

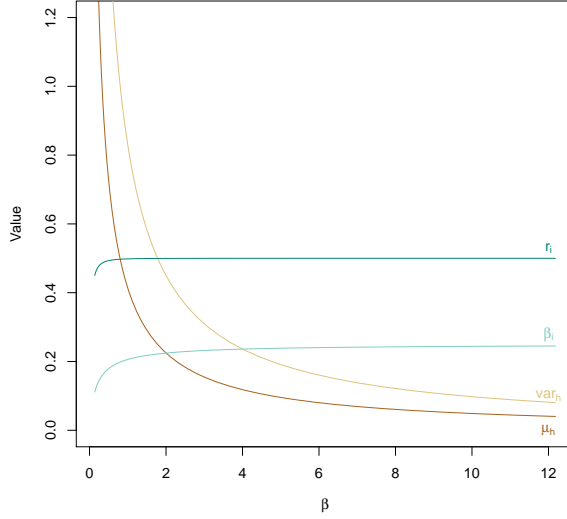


Figure 1: Limit of site updates under increasing cavity precision. We use the example given by eq. (14), where the site is a logistic likelihood, the cavity prior has mean 0 and precision β . The quantities shown are: the mean and variance of h_i (labeled μ_h and var_h), and the site parameters r_i and β_i . As expected, the mean tends to 0, and the variance tends to β^{-1} . More surprisingly, the site parameters have non-trivial limits that can be computed exactly (see main text).

We can now state our result formally. For simplicity, the case we have just discussed had increasing precision and a fixed mean. The following theorem is stated in a slightly more general case in which the cavity mean is slightly offset from μ_0 , but tends to it in as $\beta \rightarrow +\infty$. This more general case is important for the corollaries we derive from this theorem.

Theorem 1. *Limit behavior of hybrid distributions*

Consider the hybrid distribution: $h_i(x) = l_i(x) \exp\left(-\frac{\beta}{2}x^2 + (\beta\mu_0 - \delta r)x\right)$. In the limit that $\beta \rightarrow \infty$, the natural parameters of its Gaussian approximation converge to:

$$\begin{aligned} var_{h_i}^{-1} E_{h_i} &\approx var_{h_i}^{-1} \mu_0 - \delta r + \phi'_i(\mu_0) \\ var_{h_i}^{-1} &\approx \beta + \phi''_i(\mu_0) \end{aligned}$$

Thus, the natural parameters of the EP approximation ($r_i = var_{h_i}^{-1} E_{h_i}(x) - (\beta\mu_0 - \delta r)$ and $\beta_i = var_{h_i}^{-1} - \beta$) of l_i converge:

$$\begin{aligned} r_i &= -\phi'_i(\mu_0) + \beta_i \mu_0 + \mathcal{O}\left(\beta^{-1} + \left|\delta r + \phi'_i(\mu_0)\right| \beta^{-1}\right) \\ \beta_i &= \phi''_i(\mu_0) + \mathcal{O}\left(\beta^{-1} + \left|\delta r + \phi'_i(\mu_0)\right| \beta^{-1}\right) \end{aligned}$$

Note the important role of the δr term: it causes the cavity-mean to be slightly different from μ_0 , but it can accelerate convergence when set precisely to $\delta r = -\phi'_i(\mu_0)$ (see appendix).

Proof. We only give a sketch of the proof here, because it is too long and involved.

Our proof can be understood as simply computing the asymptotic behavior of $E_{h_i}(x)$ and $var_{h_i}(x)$. The first order is easily found to be: $E_{h_i}(x) \approx \mu_0$ and $var_{h_i}(x) \approx \beta^{-1}$. However, when we compute the new values for r_i and β_i , the subtraction of the cavity parameters effectively cancels that first order term. In our proof, we thus go beyond the first order and compute the next order which gives us the claimed bound.

In practice, we use two tricks that enable us to directly express β_i and r_i as expected values under the hybrid h_i , which saves us from actually computing the limit behavior of the mean and variance. We then approximate these expected values using Taylor expansions and get the claimed result. See the appendix for details. \square

2.2.2 Limit behavior of parallel-EP and aEP.

Now that we have some handle on the behavior of site-updates, we can start to study the behavior of the algorithm as a whole. A full step of aEP or parallel EP is a combination of n site updates, and that is what we characterize next. We show that one step of parallel-EP or of one step of aEP both converge towards the result of one step of Newton's algorithm. It is also possible to use Theorem 1 to describe the limit behavior of sequential-EP or of an EP variant which updates batches of sites sequentially, which tend to variants of Newton's³. We choose to focus on parallel-EP because its limiting behavior is classic Newton's.

Let's first present the limit behavior of aEP, which is easier to visualize because it only has two parameters instead of $2n$ -parameters like EP. One interesting feature of the limit behavior of the site-update is that the value of the cavity precision β_{-i} does not influence the limit behavior, which is only set by the cavity mean μ_{-i} . In the aEP algorithm, the cavity mean is always equal to the current approximation mean. Thus, when we sum all r_i and β_i approximations, we find that the limit behavior of the aEP update also has that feature: the approximation at the next step mostly depends on the current mean of the approximation, and corresponds to a Newton's update.

The limit behavior of EP is similar, but is a little more complicated to state. This is due to two additional complications. The first complication is that, in EP, each cavity mean μ_{-i} is slightly different. This is where the δr parameter from Theorem 1 comes into play: it enables us to see each cavity distribution instead as almost centered at the same mean but slightly offset in a specific direction. The second complication is that, whereas in aEP each cavity distribution has the same precision, once again each cavity distribution is different in EP. In the end, these complications hardly matter for the limit behavior, but they do make it slightly harder to understand how EP works.

Theorem 2. Limit behavior of aEP and EP

Consider a current EP approximation $(r_i, \beta_i)_{i \in [1, n]}$ and the corresponding aEP approximation $(r = \sum r_i, \beta = \sum \beta_i)$ whose current mean is $\mu_0 = \frac{\sum r_i}{\sum \beta_i}$. In the limit that all cavity-precisions $\beta_{-i} = \sum_{j \neq i} \beta_j$ tend to infinity (so that $\min(\beta_{-i})$ is of same order as β), the limit behavior of one step of aEP and of one step of EP is identical to Newton's algorithm.

For aEP, the global parameters at the next step are:

$$\begin{aligned} r_{\text{aEP}} &= -\psi'(\mu_0) + \beta_{\text{aEP}} \mu_0 + \mathcal{O}\left(n\beta^{-1} + \sum_i |\phi'_i(\mu_0)| \beta^{-1}\right) \\ \beta_{\text{aEP}} &= \psi''(\mu_0) + \mathcal{O}\left(n\beta^{-1} + \sum_i |\phi'_i(\mu_0)| \beta^{-1}\right) \end{aligned}$$

For EP, the global parameters at the next step are:

$$\begin{aligned} \sum_i r_i^{\text{new}} &= -\psi'(\mu_0) + \left(\sum_i \beta_i^{\text{new}}\right) \mu_0 + \mathcal{O}\left(n\beta^{-1} + \sum_i |r_i - \beta_i \mu_0 + \phi'_i(\mu_0)| \beta^{-1}\right) \\ \sum_i \beta_i^{\text{new}} &= \psi''(\mu_0) + \mathcal{O}\left(n\beta^{-1} + \sum_i |r_i - \beta_i \mu_0 + \phi'_i(\mu_0)| \beta^{-1}\right) \end{aligned}$$

Proof. This result is simply obtained by summing the approximations offered by Theorem 1.

For aEP, this is simple enough: all the cavity distributions are Gaussians with precision $\frac{n-1}{n}\beta$ and with mean μ_0 . Straightforward application of theorem 1 leads to the claimed result.

For EP, this is more complicated since every cavity distribution is different. However, it is straightforward to check that the cavity densities are:

$$g_{-i}(x) \propto \exp\left[-(\beta - \beta_i) \frac{x^2}{2} + ((\beta - \beta_i) \mu_0 + \beta_i \mu_0 - r_i) x\right]$$

We can then apply theorem 1 with cavity precision $\beta - \beta_i$ and offset $\delta r = r_i - \beta_i \mu_0$, and recover the claimed result. \square

³For example, sequential EP would asymptote to a variant of sequential gradient descent with a Hessian correction. See Oppen (1998) for a more extensive discussion of the link between sequential EP and sequential gradient descent.

2.3 Where to find EP’s fixed points

In this section, we use the results above to find out more about the location of fixed points of EP and aEP. We show that wherever the posterior distribution has a strongly peaked mode, a fixed point of EP or aEP lies in the vicinity. Our proof relies on an application of Brouwer’s fixed point theorem, and relies on finding *stable regions* of the parameter space, in a sense we need to make precise.

Since Newton’s iterations are strongly contractive towards posterior modes, and since our results tell us that the iterations of EP and aEP are not far from those of Newton’s, there is a good chance EP and aEP do not stray too far from posterior modes either. Indeed, we prove that there exist compact regions of the parameter space near the CGA which are stable under the aEP or the EP updates: i.e., if we start from inside of them, we stay inside. We can picture these stable regions as boxes in parameter spaces inside of which aEP and EP get stuck.

Unfortunately, our bounds are too weak to guarantee that the iterations of aEP and EP converge in such regions. We know that they cannot exit the box, but we cannot prove that they do not wander around forever inside of it. However, there is a much more interesting consequence of the existence of such stable regions: from the Brouwer fixed-point theorem, we know that any compact stable region must contain at least one fixed-point of the corresponding iteration, and so we have boxes in parameter spaces that contain both a fixed point of Newton’s and a fixed point of aEP/EP. In order to apply this insight, we would then want to find stable regions that are as small as possible in order to give the tightest bounds on the position of that fixed-point.

In this section, we focus on identifying stable regions that are a close neighborhood of the CGA at the mode of the target distribution, and we compute the correct asymptotic scaling of the size of the stable region. These results are sufficient to prove that aEP and EP are both exact in the large-data limit. However, it would be an interesting extension of the present work to also find maximal stable regions, and to find “unstable” regions: regions of the parameter space that the EP iteration is guaranteed to leave and which therefore cannot hold a fixed-point.

We find that all modes of $p(x)$ have the potential to have an associated stable region, and that the size of that stable region depends on log-curvature at the mode: more peaked modes have an associated region that is smaller than flatter modes. We use this result in the next section to prove that aEP and EP fixed points converge to the CGA at the mode in the large-data limit.

We use aEP to outline this result. Let’s assume that the starting global approximation is in close proximity to the CGA at a mode x^* of $p(x)$:

$$\begin{aligned} |r_{aEP} - \beta_{aEP} x^*| &\leq n\Delta_r \\ |\beta_{aEP} - \psi''(x^*)| &\leq n\Delta_\beta \end{aligned}$$

By applying Theorem 1 to a Gaussian approximation centered at x^* , we find that the new value of the aEP parameters are such that $r_{aEP}^{new} - \beta_{aEP}^{new} x^*$ is small:

$$r_{aEP}^{new} - \beta_{aEP}^{new} x^* = \mathcal{O} \left(n \left[\psi''(x^*) - \Delta_\beta \right]^{-1} + \left[n\Delta_r + \sum_i |\phi'_i(x^*)| \right] \left[\psi''(x^*) - \Delta_\beta \right]^{-1} \right) \quad (15)$$

If the error is smaller than $n\Delta_r$, the initial region would be stable in r . In order to find the limits of the stable region, we simply need to find values Δ_β and Δ_r for which we can guarantee that the error is strictly smaller. Inspection of eq. (15) suggests immediately that the curvature at the mode (represented by $\psi''(x^*)$) plays a key role: the larger the curvature, the tighter the bound.

For EP, the stable regions take the form:

$$\begin{aligned} |r_i + \phi'_i(x^*) - \beta_i x^*| &\leq \Delta_r \\ |\beta_i - \phi''_i(x^*)| &\leq \Delta_\beta \end{aligned}$$

which ensures the global approximation is inside stable regions with the same form as those for aEP.

Δ_r and Δ_β are small if the log-curvature at the mode is sufficiently high, as summarized by the following theorem:

Theorem 3. *Convergence of fixed points of EP and aEP*

There exists an EP and an aEP fixed-point close to the CGA of $p(x)$ at x^* if $\phi_i''(x^*)$ is sufficiently large. More precisely, if:

$$\begin{aligned}\delta_{aEP} &= \max(K_3, K_4) \sum |\phi_i'(x^*)| \left[\psi''(x^*) \right]^{-1} \\ \delta &= n \max(K_3, K_4) \left[\psi''(x^*) \right]^{-1}\end{aligned}$$

are $\mathcal{O}(1)$ quantities and $\psi''(x^*)$ is large, then the limit of the stable regions on the global approximation, $n\Delta_r$ and $n\Delta_\beta$, scale as $\mathcal{O}(\delta_{aEP} + \delta)$ for aEP and as $\mathcal{O}(\delta)$ for EP.

Proof. We only sketch the proof of this theorem which we detail in the appendix. We focus on the simpler aEP case but the reasoning is identical for EP.

The key idea is the following: if we perform a first order perturbation in r_{aEP} or in β_{aEP} while β_{aEP} is large, then this perturbation has a negligible effect on the limit behavior. Thus, the error still scales (almost) as if we were starting from the CGA at x^* : $\beta_{aEP} = \psi''(x^*)$ and $r_{aEP} = \beta_{aEP}x^*$:

$$\begin{aligned}r_{aEP}^{new} &= \beta_{aEP}^{new}x^* + \mathcal{O}\left(n \max(K_3, K_4) \left[\psi''(x^*) \right]^{-1}\right) \\ \beta_{aEP}^{new} &= \psi''(x^*) + \mathcal{O}\left(\max(K_3, K_4) \left[n + \sum_{i=1}^n |\phi_i'(x^*)| \right] \left[\psi''(x^*) \right]^{-1}\right)\end{aligned}$$

from which we get the claimed limit behavior. □

Remark. It might seem strange to refer to δ and δ_{aEP} as “order 1” quantities. This holds in the large-data regime as we show in the next section, but an easier example to visualize is the following. Consider the EP approximation of a fixed-probability distribution raised to power λ : $[p(x)]^\lambda = \prod_i [l_i(x)]^\lambda$. For that example, as $\lambda \rightarrow \infty$, $\lambda\psi''(x^*) \rightarrow \infty$: the log-derivative at the mode grows linearly. However, the third and fourth log-derivatives also grow linearly so that $\delta = n \max(K_3, K_4) \left[\psi''(x^*) \right]^{-1}$ does not depend on λ : it is indeed of order 1. δ_{aEP} is similarly found to be of order 1.

This theorem shows two interesting features of the behavior of EP. First of all, we see that if $p(x)$ is a multimodal distribution where multiple modes are sufficiently peaked and they are sufficiently separated, then EP and aEP both have multiple fixed points, and those fixed points do not give a global account of $p(x)$ but only fit the local shape of $p(x)$ around “their” mode. This is quite contrary to the common view on EP which holds that since EP’s stated target is to find an approximation of the minimizer of $KL(p, q)$, it gives global approximations of the target distribution. We discuss this point further in section 3.2.

2.4 Large-data limit behavior

So far, all of our results have been deterministic: assuming some fixed target distribution $p(x)$, we have bounded the distance between the result of the aEP and EP updates and the result of the NT updates. We then used those results to derive a deterministic result on the possible positions of the aEP and EP fixed points. We have discussed asymptotic results in those sections in terms of either asymptotes of the parameter space (large precision β) or of properties of the target distribution (large log-curvature at a mode $\psi''(x^*)$).

In this section, we adopt a different point of view: we seek a large-data limit result. In other words, we assume that some random process is generating the sites $l_i(x)$ and we consider what happens as more and more sites are generated. In real applications, this would correspond to accumulating data of some kind and computing the posterior of the unknown x under some (most likely miss-specified) generative model. We abstract all those complications away and simply treat the l_i functions (or, equivalently, the ϕ_i functions) as function-valued random variables.

Throughout this section, the number of sites, n , is variable. We note $p_n(x)$ the random variable of the posterior distribution constructed from the n first sites $l_i(x)$. We note x_0 the minimum of $x \rightarrow E(\phi_i(x))$: x_0 can be thought of as the “true” value that we seek to recover. We note x_n^* the mode of $p_n(x)$ closest to x_0 and $q_n(x)$ the CGA of $p_n(x)$ at x_n^* .

In order for EP to have good behavior, we require the process generating the l_i to obey our assumptions on the l_i (eqs. (12) and (13)) and to obey two additional conditions. The first condition is that the distribution of the log-sites $\phi_i(x)$ is non-degenerate so that a number of variances are finite and we can apply the law of large numbers (see appendix for details). This is a mild condition and, in the rare occasion where it does not apply, we could even weaken it. This

condition ensures that the log-posterior $\sum \phi_i(x)$ is Locally Asymptotically Normal (LAN, Kleijn et al. (2012)). Under this LAN behavior, we prove that every global approximation in the aEP and EP stable regions around x_n^* converge in KL divergence and in total-variation towards the CGA at x_n^* : $q_n(x)$.

Furthermore, if the process generating the l_i produces a concentration of the mass of the posterior around x_0 , then, combined with the LAN behavior of the posterior, we have enough to guarantee that the posterior $p_n(x)$ converges towards its CGA $q_n(x)$ in total-variation. This result is the last we need to prove that, in the large-data limit, aEP and EP are exact in the following sense: there is a large neighborhood of aEP and EP approximations that surrounds at least one fixed-point and where the aEP and EP iterations are “stuck”, such that all approximations in the neighborhood are asymptotically exact.

The technical condition we require for concentration of mass is the following: for all $\epsilon > 0$, the integrals $\int p_n(x) 1(|x - x_0| \leq \epsilon) dx$, which are random variables whose distribution is dictated by the distribution of the $l_i(x)$, need to converge in probability to 1. In other words, for every $\epsilon > 0$, the posterior is guaranteed to concentrate inside the ϵ -ball centered around x_0 . This should be thought of as an identifiability condition: it requires the posterior to concentrate around the “true” parameter value x_0 .

Theorem 4. *aEP and EP are exact in the large-data limit.*

Under our assumptions on the sites and the site-generating process, all Gaussian distributions in the stable region of th. 2 converge in total-variation to the CGA q_n with probability 1. The convergence rate is $\mathcal{O}(n^{-1/2})$.

Under a further identifiability assumption, all Gaussian distributions in the stable region converge in total-variation to p_n with probability 1. The convergence rate is $\mathcal{O}(n^{-1/2})$.

Proof. Here is a sketch of the proof. First, define $I_0 = E(\phi_i''(x_0))$ the Fisher information of our likelihood-generating process.

By a law of large numbers argument, $\sum_{i=1}^n \phi_i''(x_0) \approx nI_0$: this quantity grows linearly. In the meantime, the gradient at x_0 is small: $\sum_{i=1}^n \phi_i'(x_0) \approx \sqrt{n} \sqrt{\text{var}(\phi_i'(x_0))}$. Combining this with the third derivative bound and a simple Taylor expansion of $\sum_{i=1}^n \phi_i'(x_0)$ proves that there must be a mode of p_n : x_n^* , in close proximity to x_0 . The distance between the two scales as: $x_n^* - x_0 = \mathcal{O}(1/\sqrt{n})$.

Since the log-curvature at x_0 grows linearly and $x_0 - x_n^* = \mathcal{O}(1/\sqrt{n})$, the log-curvature at x_n^* also grows linearly:

$$\sum_{i=1}^n \phi_i''(x_n^*) \approx nI_0$$

Similarly, $\sum_{i=1}^n |\phi_i'(x_n^*)|$ grows linearly and $n \max(K_3, K_4)$ trivially grows linearly with n . Thus, the conditions of th. 2 are checked: there exists a stable region near the CGA at x_n^* which holds at least one fixed-point for aEP and EP.

To prove the total-variation convergence, we actually prove a KL-divergence convergence. The bounds on Δ_r and Δ_β translate into a $\mathcal{O}(n^{-1})$ KL-divergence bound. From Pinsker’s inequality, this translates into a $n^{-1/2}$ total-variation bound.

The proof then concludes by proving a $n^{-1/2}$ convergence of the CGA towards p_n which is a simple application of a Bernstein-von Mises theorem for miss-specified models by Kleijn et al. (2012). \square

As a corollary from this theorem, it follows that EP is asymptotically exact in all models which respect our hypothesis on the l_i and the l_i -generating process and which are identifiable. This includes an extremely large class of models since our conditions are fairly mild and since identifiability is a key requirement for the Bayesian method to be useful. For example, our result can be applied to both probit and logistic regression in finite-dimensions, as long as the feature vectors are bounded (in order for our hypotheses on the l_i to be verified), and spread uniformly enough for the Fisher information matrix to be strictly positive (see Appendix). Three notes must be made on that theorem.

First of all, it shows that EP and aEP are exact in that there exists a fixed-point which converges in total-variation to the true posterior. It does not guarantee that asymptotically all fixed points converge. In particular, should the expected value of $\phi_i(x)$ have several modes, we can guarantee that there also exists aEP and EP fixed points which are terrible asymptotic approximations of $p_n(x)$: the stable regions associated with the local minima converge to the CGA at a mode with negligible asymptotic contribution to the mass of p_n .

Second, it could seem from this result that EP and aEP approximations are asymptotically worse than the CGA, because the total-variation distance between the EP fixed-point and the target decreases slower than for the CGA. This does not

reflect a limitation of EP but it is a feature of our proof: we have proved that EP is good because it converges to the CGA, and only a direct proof would be able to prove the superiority of EP. We expect that EP should give better asymptotic approximations than the CGA from empirical tests of both methods, but the result we present here is too weak to prove this conjecture. We have recently made some progress on such a direct proof, but under more restrictive assumptions than the ones presented here (Dehaene and Barthelmé, 2015).

Finally, it is interesting to come back to th. 2 which shows that, in the large cavity precision limit, aEP and parallel EP converge to NT. It is also possible to qualitatively discuss th. 2 in terms of a large-data limit instead. In order to do so, we assume that, as the number of data-points grows, the typical value for the cavity precisions β_{-i} grows linearly with n . This is certainly true in the stable region around x_0 as we have just shown in th. 4. If we have that $\min(\beta_{-i}) \propto n$, then the errors in th. 2 are of order 1. These order 1 errors are negligible in the large-data limit, in exactly the same way as for th. 4. Thus our result that aEP and parallel EP are almost Newton in the high precision limit qualitatively apply in the large-data limit as long as the “typical” cavity precisions grow linearly with n .

3 Consequences of the quasi-Newton behavior of EP

In the previous section, we gave a proof that, in the limit of large-data, EP behaves like a Newton search for the mode of the target distribution. In this section, we highlight how this result can inform our intuition about how EP behaves, and some potentially interesting avenues of research it opens.

3.1 Instability of the EP iteration

Newton’s algorithm (NT) is a good tool in finding a mode of a target distribution as it has fast convergence if it is initialized properly (i.e.: close enough to the mode), but it can often fail to converge globally. For example, applying NT to $f(x) = \exp(-|x|^{4/3})$ always results in a divergent sequence that oscillates wildly around the fixed point at $x = 0$. More generally, Newton is unstable when the log-curvature ψ'' is small because that makes the Newton step $[\psi'']^{-1} \psi'$ too big.

In order to fix this problem, it is necessary to introduce a “slowed-down” version of the iteration:

$$\mu_{t+1} = \mu_t - \gamma_t \frac{\psi'(\mu_t)}{\psi''(\mu_t)}$$

where $0 \leq \gamma_t \leq 1$ is chosen carefully to ensure convergence. As the NT algorithm is part of the class of Generalized Gradient Descent algorithms, one solution is to choose values γ_t that respect the Wolfe conditions (see Boyd and Vandenberghe, 2004, for a convergence analysis of Newton’s method).

Since EP behaves like NT in the large-data limit, we can intuit that even for small n , EP might have a qualitatively similar behavior. In particular, EP iterations might oscillate around their fixed-point just like NT does. We give here a simple example of this behavior with sites that are extremely regular and which seem harmless at a glance.

In our example, we applied a parallel version of the EP algorithm to the following situation:

- five “double-logistic” sites: $\forall i \in \{1, \dots, 5\}$, $l_i(x) = (1 + \exp(5x))^{-1} (1 + \exp(-5x))^{-1}$, so called because they are the product of two logistic functions. If plotted, these appear to be Gaussian at a glance, but with the important difference that they only have exponential decay in their tails. In these exponential tails, the log-curvature $\phi_i''(x)$ is very small.
- one Gaussian site representing a prior: $l_0(x) = \exp(-x^2/2)$

In this example, there is an EP fixed-point that provides a good approximation of the target distribution. However, we also found that the EP iteration is unstable if it is initialized too far away from the fixed-point distribution. EP iterations initialized too far away converge to a limit cycle oscillating between two approximations that are completely wrong. Figure 2 shows the basins of attraction of the stable equilibrium and the limit cycle, and one example trajectory for each.

Our results on the limit behavior of the EP iteration can thus inform our understanding of why the EP iteration sometimes has problems with convergence: it could be that the EP iteration overshoots when it is operating in a zone where most $\phi_i''(x)$ are small while most $\phi_i'(x)$ are big, exactly like NT would. A possible solution to this could be to complement EP with an adaptive step algorithm. This algorithm would need to detect overshoots or potential overshoots, and prevent them. Finding such an adaptive step algorithm would represent major progress in EP methods.

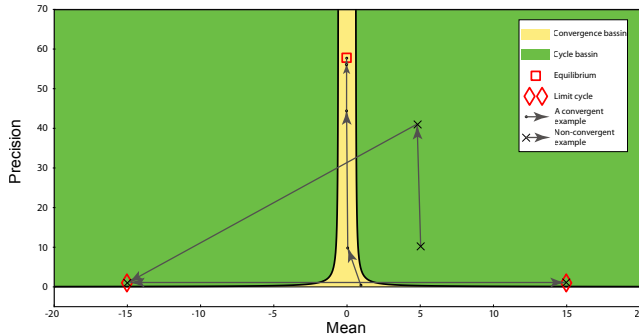


Figure 2: Convergence of aEP on double-logistic sites. We evaluated the stability of the averaged-EP algorithm on five double-logistic sites and one Gaussian prior site. The aEP iteration either converged to a fixed point (red square) or to an oscillation (between the two red diamonds). The yellow background corresponds to the basin of attraction of the fixed point and the green background to that of the limit cycle. The first four steps of the aEP iteration are presented for two initial points, one in each basin. Note how fast the convergence to both attractors is: in four steps, the iteration reaches a very close neighborhood of the attractors.

3.2 Behavior of EP on multimodal distributions

Let’s now investigate how our results shed new light on the behavior of EP on a multimodal target distribution $p(x)$.

EP has been presented from the start as a rough approximation to the minimizer of the “forward” KL divergence: $KL(p||q)$ that uses local (i.e., site-specific) approximations of the KL divergence. This leads to the intuition that, when applied on a multimodal target, the EP approximation would fit all modes, or maybe most modes, since this is the behavior of the KL approximation.

With our method of bounding fixed points in neighborhoods of the CGA at the various modes of $p(x)$, we can now see that this intuition is flawed. Indeed, our result shows that all modes that are:

- sufficiently peaked, so that the stable region is small
- sufficiently isolated, so that their stable region does not overlap with that of the other modes

have at least one associated fixed-point. This fixed-point corresponds to the EP approximation fitting only this mode and not the rest of the probability distribution. Thus, it can happen that EP approximations give only a partial account of the target distribution.

However, it’s also false to believe that EP always gets captured and never provides a global approximation of a multimodal target. Indeed, when there is only one site (or more generally, when there is only a few sites), EP does give a global account of the distribution since EP with one site exactly recovers the KL approximation of $p(x)$.

Surprisingly, both types of fixed points can co-exist. Figure 3 shows an example involving Gaussian mixtures, the prototypical example of multimodal problems. Here the data $y_1 \dots y_n$ are supposed IID, with

$$p(y_i|\mathbf{x}) = \frac{1}{2} (\mathcal{N}(y_i; x_1, 1) + \mathcal{N}(y_i; x_2, 1))$$

The parameters correspond to component means in the Gaussian mixture and are evidently interchangeable, so that the likelihood surface is in general bimodal. We ran EP in this example with $n = 20$, $\mathbf{x} = (0, -2.5)$ and a unit Gaussian prior on \mathbf{x} . Different initializations lead to different fixed points: we found three, two corresponding to local approximations (as predicted by theory) and a global one, the latter far from any mode. Interestingly, the local approximations are locally “exact”, meaning that under the identifiability constraints $x_2 > x_1$, the moments of the corresponding EP approximation are exact. The mean of the global approximation matches the exact global mean, although the covariance is a bit underestimated.

A simple take-home message from our work should thus be this one: do not expect EP to fit all modes of a target distribution, but do not automatically assume that it will fit a single mode either.

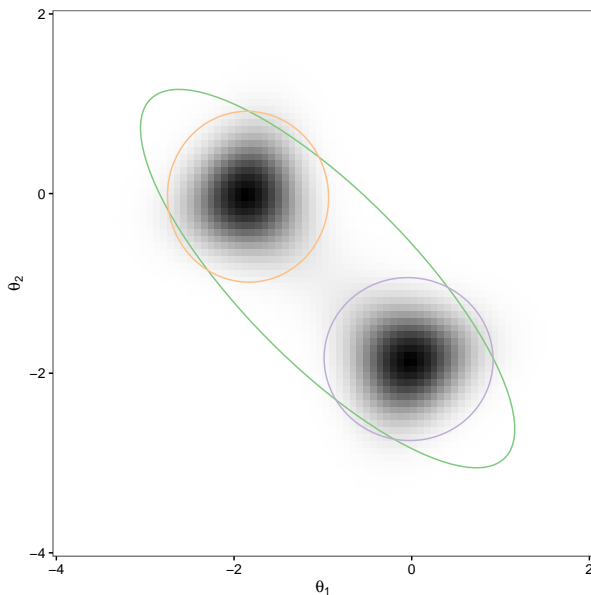


Figure 3: Behavior of EP on multimodal target distributions. The grey density represents the target, and the ellipses different EP approximations (summarised as 95% confidence regions). In this example EP has three possible fixed points, one corresponding to a global approximation of the target and the other two to local approximations. Which fixed point is reached depends on the initialisation. See text for details.

4 Conclusion

EP is an algorithm whose theoretical analysis lags far behind its empirical success. We describe in this manuscript a number of results that narrow the gap between theory and empirics, and we hope that they will provide a useful basis for future work.

In this article, we propose a simpler version of EP which we call averaged-EP or aEP. aEP could be interesting as an empirical algorithm (see Appendix and Li et al. (2015) who introduce a close variant of aEP called stochastic EP). However, our main focus is on using it as a theoretical tool for studying the asymptotics of EP, since its reduced parameter space makes the results simpler to understand. We derive analytical results on aEP and EP in several limits: in the limit of large cavity precisions, and in the classical large-data limit. We prov that both methods converge to a Newton’s search for a mode of the target distribution. We then show that both are asymptotically exact in that there exists a fixed-point which converges towards the target.

Our theoretical results open several avenues of research into gaining a better understanding of EP. First of all, while we shed some light into the behavior of the EP iterations by providing a qualitative link to Newton’s method, we still do not know how to build a variant of EP which is guaranteed to converge. This is a key avenue of research since the only way we know to guarantee convergence to an EP fixed-point, the Expectation-Consistent algorithm (Opper and Winther, 2005), converges much more slowly. An algorithm that always converges while staying as fast as EP would represent a major step forward. The parallel with NT opens the interesting idea of designing a line-search extension of EP.

Another limit of our result is the coarseness of our bounds: while we show that EP is asymptotically exact, we do not show that it improves on the Canonical Gaussian Approximation when there is ample empirical evidence that it does. Future theoretical work on EP should aim at showing how and when EP does dominate the CGA (see Dehaene and Barthelmé (2015) for one such investigation, though crippled by unrealistic assumptions on the model).

A final interesting extension of this work concerns the non-parametric case, and, more generally, EP approximations of high-dimensional posteriors. Indeed, we believe that our results are sub-optimal in bounding how the error scales in high-dimensional cases, which is why we cannot apply our results to the non-parametric case for which $p = n$. A careful extension to show that EP behaves correctly in those cases would prove another huge step forward in providing a good theoretical basis for EP.

Acknowledgments

We thank Alex Pouget for his support, and Hugo Duminil for helpful insight on the math. We also thank Micolisande Albert, Nicolas Chopin, Gina Gr̃oenhage, and James Ridgway for their comments on the manuscript. Finally, we thank Judith Rousseau for her help on Bernstein-von Mises theorems.

References

- Barthelmé, S. and Chopin, N. (2014). Expectation propagation for likelihood-free inference. *Journal of the American Statistical Association*, 109(505):315–333.
- Bishop, C. M. (2007). *Pattern Recognition and Machine Learning (Information Science and Statistics)*. Springer, 1st ed. 2006. corr. 2nd printing 2011 edition.
- Boyd, S. and Vandenberghe, L. (2004). *Convex Optimization*. Cambridge University Press, New York, NY, USA.
- Brascamp, H. J. and Lieb, E. H. (1976). Best constants in Young’s inequality, its converse, and its generalization to more than three functions . *Advances in Mathematics*, 20(2):151 – 173.
- Dehaene, G. P. and Barthelmé, S. (2015). Bounding errors of Expectation-Propagation. In Cortes, C., Lawrence, N. D., Lee, D. D., Sugiyama, M., and Garnett, R., editors, *Advances in Neural Information Processing Systems 28*, pages 244–252. Curran Associates, Inc.
- Gehre, M. and Jin, B. (2013). Expectation Propagation for Nonlinear Inverse Problems - with an Application to Electrical Impedance Tomography.
- Gelman, A., Vehtari, A., Jylänki, P., Robert, C., Chopin, N., and Cunningham, J. P. (2014). Expectation propagation as a way of life.
- Jylänki, P., Nummenmaa, A., and Vehtari, A. (2014). Expectation propagation for neural networks with sparsity-promoting priors. *Journal of Machine Learning Research*, 15:1849–1901.
- Jylänki, P., Vanhatalo, J., and Vehtari, A. (2011). Robust gaussian process regression with a student-t likelihood. *J. Mach. Learn. Res.*, 12:3227–3257.
- Kleijn, B., van der Vaart, A., et al. (2012). The bernstein-von-mises theorem under misspecification. *Electronic Journal of Statistics*, 6:354–381.
- Kuss, M. and Rasmussen, C. E. (2005). Assessing Approximate Inference for Binary Gaussian Process Classification. *J. Mach. Learn. Res.*, 6:1679–1704.
- Li, Y., Hernández-Lobato, J. M., and Turner, R. E. (2015). Stochastic Expectation Propagation. In Cortes, C., Lawrence, N. D., Lee, D. D., Sugiyama, M., and Garnett, R., editors, *Advances in Neural Information Processing Systems 28*, pages 2323–2331. Curran Associates, Inc.
- Minka, T. (2005). Divergence Measures and Message Passing. Technical report.
- Minka, T. P. (2001). Expectation Propagation for approximate Bayesian inference. In *UAI ’01: Proceedings of the 17th Conference in Uncertainty in Artificial Intelligence*, pages 362–369, San Francisco, CA, USA. Morgan Kaufmann Publishers Inc.
- Nickisch, H. and Rasmussen, C. E. (2008). Approximations for Binary Gaussian Process Classification. *Journal of Machine Learning Research*, 9:2035–2078.
- Nocedal, J. and Wright, S. (2006). *Numerical Optimization (Springer Series in Operations Research and Financial Engineering)*. Springer, 2nd edition.
- Opper, M. (1998). On-line Learning in Neural Networks. chapter A Bayesian Approach to On-line Learning, pages 363–378. Cambridge University Press, New York, NY, USA.
- Opper, M. and Winther, O. (2005). Expectation Consistent Approximate Inference. *J. Mach. Learn. Res.*, 6:2177–2204.

- Paquet, U., Winther, O., and Opper, M. (2009). Perturbation Corrections in Approximate Inference: Mixture Modelling Applications. *Journal of Machine Learning Research*, 10:1263–1304.
- Pereyra, M. (2016). Approximating Bayesian confidence regions in convex inverse problems.
- Raymond, J., Manoel, A., and Opper, M. (2014). Expectation propagation.
- Ribeiro, F. and Opper, M. (2011). Expectation propagation with factorizing distributions: A gaussian approximation and performance results for simple models. *Neural computation*, 23(4):1047–1069.
- Ridgway, J., Alquier, P., Chopin, N., and Liang, F. (2014). PAC-Bayesian AUC classification and scoring. In Ghahramani, Z., Welling, M., Cortes, C., Lawrence, N., and Weinberger, K., editors, *Advances in Neural Information Processing Systems 27*, pages 658–666. Curran Associates, Inc.
- Rue, H., Martino, S., and Chopin, N. (2009). Approximate bayesian inference for latent gaussian models by using integrated nested laplace approximations. *Journal of the Royal Statistical Society: Series B (Statistical Methodology)*, 71(2):319–392.
- Saumard, A. and Wellner, J. A. (2014). Log-concavity and strong log-concavity: A review. *Statist. Surv.*, 8:45–114.
- Seeger, M. (2005). Expectation Propagation for Exponential Families. Technical report.
- Titterton, D. M. (2011). The em algorithm, variational approximations and expectation propagation for mixtures. In *Mixtures*, pages 1–29. John Wiley & Sons, Ltd.
- Varadhan, R. and Roland, C. (2008). Simple and globally convergent methods for accelerating the convergence of any em algorithm. *Scandinavian Journal of Statistics*, 35(2):335–353.
- Wainwright, M. J. and Jordan, M. I. (2008). *Graphical Models, Exponential Families, and Variational Inference (Foundations and Trends(r) Machine Learning)*. Now Publishers Inc.
- Xu, M., Lakshminarayanan, B., Teh, Y. W., Zhu, J., and Zhang, B. (2014). Distributed bayesian posterior sampling via moment sharing. In *Advances in Neural Information Processing Systems*, pages 3356–3364.

Supplementary information

The following two sections hold all the supplementary information of this article.

5 Proofs

In this section, we will give detailed proofs of all the results we have presented in the main text.

We will prove, in order:

1. the limit behavior of the EP update in one-dimension
2. the limit behavior of the EP update in high-dimensions
3. the limit behavior under weaker assumptions
4. the exactness of aEP and EP in the large-data limit

5.1 Assumptions

We will prove our results in the one-dimensional case and in the n-dimensional case. Let's first recall our assumptions on the likelihoods in the one-dimensional case. We will explain in section 5.3 how to modify these assumptions in the high-dimensional case. In section 5.4, we show that these assumptions can be weakened considerably, though the expression for the errors is much harder to state.

Let $l_i(x) = \exp(-\phi_i(x))$ be the sites, and $\phi_i(x)$ be the negative log of each site.

Our first assumption will be that the second log-derivatives of the sites span a finite range:

$$\max(\phi_i''(x)) - \min(\phi_i''(x)) \leq B \quad (16)$$

and second, that some of the higher log-derivatives are bounded. There exists constants K_d for $d \in [3, 4]$ such that:

$$|\phi_i^{(d)}(x)| \leq K_d \quad (17)$$

5.2 Limit behavior of the EP update

In this section, we will prove the following theorem.

Theorem 5. *Limit behavior of the site-approximation*

Consider the hybrid distribution: $h_i(x) = l_i(x) \exp\left(-\frac{\beta}{2}x^2 + (\beta\mu_0 - \delta r)x\right)$. In the limit that $\beta \rightarrow \infty$, the hybrid mean $E_{h_i}(x)$ and the natural parameters of the EP approximation ($r_i = \text{var}_{h_i}^{-1} E_{h_i}(x) - (\beta\mu_0 - \delta r_i)$ and $\beta_i = \text{var}_{h_i}^{-1} - \beta$) of l_i converge. Defining $K_M = \max(K_3, K_4)$ and $\Delta_r = (\phi_i'(\mu_0) + \delta r)$, the limits are:

$$\begin{aligned} E_{h_i}(x) = \mu_{h_i} &= \mu_0 + \mathcal{O}(\Delta_r \beta^{-1} + K_M \beta^{-2}) \\ r_i &= \beta_i \mu_{h_i} - E_{h_i}(\phi_i'(x)) \\ &= -\phi_i'(\mu_0) + \beta_i \mu_0 + \mathcal{O}(K_M \beta^{-1} + K_M \beta^{-1} [\mu_{h_i} - \mu_0] + K_M [\mu_{h_i} - \mu_0]^2) \\ &= -\phi_i'(\mu_0) + \beta_i \mu_0 + \mathcal{O}(K_M \beta^{-1} + \beta^{-2}) \\ \beta_i &\approx E_{h_i}(\phi_i''(x)) \\ &= \phi_i''(\mu_0) + \mathcal{O}(K_M \beta^{-1} + K_M [\mu_{h_i} - \mu_0]) \\ &= \phi_i''(\mu_0) + \mathcal{O}(K_M \beta^{-1} + K_M \Delta_r \beta^{-1}) \end{aligned}$$

Remark. Note the key role of the δr parameter. It causes the mean of the cavity distribution to be offset from μ_0 , but it can make the mean of the hybrid, μ_{h_i} , closer to μ_0 . Indeed, if δr is such that $\Delta_r = 0$, then we gain an order of magnitude in the limit behavior of μ_{h_i} and the errors in the limit behavior of both r_i and β_i are smaller.

Proof. Let's first sketch a global overview of how the proof works. Intuitively, what is going on is that we are going beyond the first order approximations of the mean and variance of h_i :

$$\begin{aligned} E_{h_i}(x) &\approx \mu_0 \\ \text{var}_{h_i}(x) &\approx \beta^{-1} \end{aligned}$$

and computing the next order of their limit behavior. If we try to follow that path directly, however, we obtain bounds that are a bit ugly and not very tight. A better proof path is slightly clever and sophisticated and consists in finding "tricks" ways to bound β_i and r_i directly. This is where the Brascamp-Lieb inequality comes in play: it provides one-half of the β_i bound.

In practice, our proof can be decomposed into five steps:

- Upper-bound $\text{var}_{h_i}(x)$ in a coarse way
- Upper-bound and lower-bound $\text{var}_{h_i}(x)$ in a fine way

- Prove a coarse bound on the $E_{h_i}(x) - \mu_0 = \mu_{h_i} - \mu_0$ from the coarse bound on the variance
- Use the bound on $\mu_{h_i} = E_{h_i}(x)$ to improve the bound on $\text{var}_{h_i}(x)$ to its final state which provides us with the bound on β_i
- Compute the limit behavior of r_i from the coarse limit behavior of $\text{var}_{h_i}(x)$ and μ_{h_i}

Limit behavior of $\text{var}_{h_i}(x)$ and of $\beta_i = \text{var}_{h_i}(x)^{-1} - \beta$ First, we will deal with the variance of the hybrid. We will use the Brascamp-Lieb result and a Cramer-Rao like bound to derive the final bounds on β_i . The Brascamp-Lieb result will also give a coarse bound on var_{h_i} which we will use in the other sections.

Let's start by upper-bounding the variance with the Brascamp-Lieb bound. This will also give us the coarse bound we need on $\text{var}_{h_i}(x)$.

Consider the value of ϕ_i'' at μ_0 . It gives us a universal lower-bound on $\phi_i''(x)$ (from assumption 16):

$$\phi_i''(x) \geq \phi_i''(\mu_0) - B$$

Thus, when the cavity-precision β is sufficiently large, the hybrid distribution h_i is strongly log-concave: its second log-derivative is lower-bounded everywhere by a strictly positive quantity:

$$-\frac{\partial^2}{\partial x^2} \log(h_i(x)) = \phi_i''(x) + \beta \geq \phi_i''(\mu_0) + \beta - B$$

For log-concave distributions, the variance of any statistic is upper-bounded by the Brascamp-Lieb inequality. In particular, the variance is upper-bounded by:

$$\text{var}_{h_i}(x) \leq E_{h_i} \left(\left[\phi_i''(x) + \beta \right]^{-1} \right) \quad (18)$$

From this and the curvature lower-bound, we get a coarse upper-bound on the variance:

$$\begin{aligned} \text{var}_{h_i}(x) &\leq \left[\phi_i''(\mu_0) + \beta - B \right]^{-1} \\ &\leq \mathcal{O}(\beta^{-1}) \end{aligned} \quad (19)$$

This coarse upper-bound is the first step of our proof.

Now that this coarse bound is established, we continue working on $\text{var}_{h_i}(x)$ and backtrack to eq. 18 which we will simplify. In order to simplify it, we will use several properties of the inverse function: $M \rightarrow M^{-1}$ for $M \in [\phi_i''(\mu_0) + \beta - B, \phi_i''(\mu_0) + \beta + B]$.

First, we can perform a simple Taylor expansion of the inverse function around $E_{h_i}(\phi_i''(x)) + \beta$ in order to simplify $[\phi_i''(x) + \beta]^{-1}$:

$$\begin{aligned} \left[\phi_i''(x) + \beta \right]^{-1} &\approx \left[E_{h_i}(\phi_i''(x)) + \beta \right]^{-1} \\ &\quad - \left[E_{h_i}(\phi_i''(x)) + \beta \right]^{-2} \left(\phi_i''(x) - E_{h_i}(\phi_i''(x)) \right) \\ &\quad + \left[E_{h_i}(\phi_i''(x)) + \beta \right]^{-3} \left(\phi_i''(x) - E_{h_i}(\phi_i''(x)) \right)^2 \end{aligned} \quad (20)$$

This expression is a rough approximation with which it is hard to do rigorous mathematics. We would like to replace it with an upper-bound. Thankfully, the inverse function $M \rightarrow M^{-1}$ is convex and its curvature is bounded over the interval of interest: $M \in [\phi_i''(\mu_0) + \beta - B, \phi_i''(\mu_0) + \beta + B]$. We can then upper-bound it by a second degree Taylor expansion in which we replace $\left[E_{h_i}(\phi_i''(x)) + \beta \right]^{-3}$ by an upper-bound $\left[\phi_i''(\mu_0) + \beta - B \right]^{-3}$. This yields:

$$\begin{aligned} \left[\phi_i''(x) + \beta \right]^{-1} &\leq \left[E_{h_i}(\phi_i''(x)) + \beta \right]^{-1} \\ &\quad - \left[E_{h_i}(\phi_i''(x)) + \beta \right]^{-2} \left(\phi_i''(x) - E_{h_i}(\phi_i''(x)) \right) \\ &\quad + \left[\phi_i''(\mu_0) + \beta - B \right]^{-3} \left(\phi_i''(x) - E_{h_i}(\phi_i''(x)) \right)^2 \end{aligned} \quad (21)$$

We can now get an upper-bound for the variance by combining this upper-bound (21) and the Brascamp-Lieb inequality eq. (18):

$$\begin{aligned}
\text{var}_{h_i}(x) &\leq E_{h_i} \left(\left[\phi_i''(x) + \beta \right]^{-1} \right) \\
&\leq \left[E_{h_i} \left(\phi_i''(x) \right) + \beta \right]^{-1} + \left[\phi_i''(\mu_0) + \beta - B \right]^{-3} \text{var}_{h_i} \left(\phi_i''(x) \right) \\
&\leq \left[E_{h_i} \left(\phi_i''(x) \right) + \beta \right]^{-1} + \left[\phi_i''(\mu_0) + \beta - B \right]^{-3} K_3^2 \text{var}_{h_i}(x) \\
&\leq \left[E_{h_i} \left(\phi_i''(x) \right) + \beta \right]^{-1} + K_3^2 \left[\phi_i''(\mu_0) + \beta - B \right]^{-4}
\end{aligned} \tag{22}$$

where we have bounded the variance of ϕ_i'' using a Taylor expansion, and re-used our coarse bound on the variance (19). We will now invert this expression (22). We use the convexity of the inverse function: $(a+b)^{-1} \geq a^{-1} - a^{-2}b$ (with $a = E_{h_i}(\phi_i''(x) + \beta)$) to find:

$$\begin{aligned}
\text{var}_{h_i}^{-1}(x) &\geq \left(\left[E_{h_i} \left(\phi_i''(x) \right) + \beta \right]^{-1} + K_3^2 \left[\phi_i''(\mu_0) + \beta - B \right]^{-4} \right)^{-1} \\
&\geq \left[E_{h_i} \left(\phi_i''(x) \right) + \beta \right] - K_3^2 \left[E_{h_i} \left(\phi_i''(x) \right) + \beta \right]^2 \left[\phi_i''(\mu_0) + \beta - B \right]^{-4} \\
&\geq \beta + E_{h_i} \left(\phi_i''(x) \right) - K_3^2 \frac{\left[\phi_i''(\mu_0) + \beta + B \right]^2}{\left[\phi_i''(\mu_0) + \beta - B \right]^{-4}} \\
&\geq \beta + E_{h_i} \left(\phi_i''(x) \right) - \mathcal{O}(K_3^2 \beta^{-2})
\end{aligned} \tag{23}$$

Note that in that last expression, the terms are ordered according to their asymptotic behavior: linear-term, order 1 term (which also contains a β^{-1} term) and a β^{-2} remainder.

We finally expand $\phi_i''(x)$ around $\mu_{h_i} = E_{h_i}(x)$ in order to simplify the expected value $E_{h_i}(\phi_i''(x))$:

$$\begin{aligned}
E_{h_i} \left(\phi_i''(x) \right) &\geq \phi_i''(\mu_{h_i}) - \frac{K_4}{2} \text{var}_{h_i}(x) \\
&\geq \phi_i''(\mu_{h_i}) - \frac{K_4}{2} \left[\phi_i''(\mu_0) + \beta - B \right]^{-1} \\
&\geq \phi_i''(\mu_{h_i}) - \mathcal{O}(K_4 \beta^{-1})
\end{aligned}$$

Which gives us a lower-bound for $\beta_i = \text{var}_{h_i}(x) - \beta$:

$$\begin{aligned}
\beta_i &\geq \phi_i''(\mu_{h_i}) - K_4 \left[\phi_i''(\mu_0) + \beta - B \right]^{-1} - K_3^2 \frac{\left[\phi_i''(\mu_0) + \beta + B \right]^2}{\left[\phi_i''(\mu_0) + \beta - B \right]^{-4}} \\
&\geq \phi_i''(\mu_{h_i}) - \mathcal{O}(K_4 \beta^{-1} + K_3^2 \beta^{-2})
\end{aligned} \tag{24}$$

This is not our final lower-bound on β_i because it refers to the hybrid-mean μ_{h_i} and not to the cavity-mean μ_0 . As explained in the proof outline, we will further along the way bound $\mu_{h_i} - \mu_0$. We will then be able to backtrack to our bounds on β_i which refer to μ_{h_i} and, with yet another Taylor expansion, make them use μ_0 instead.

However, before we work on μ_{h_i} , let's conclude our work on β_i . We will now upper-bound β_i which requires lower-bounding var_{h_i} .

We will make use of a Cramer-Rao inequality⁴. It reads:

$$\begin{aligned}
\text{var}_{h_i}^{-1}(x) &\leq E_{h_i} \left(\phi_i''(x) + \beta \right) \\
&\leq \beta + \phi_i''(\mu_{h_i}) + K_4 E_{h_i} \left((x - \mu_{h_i})^2 / 2 \right) \\
&\leq \beta + \phi_i''(\mu_{h_i}) + \frac{K_4}{2} \text{var}_{h_i}(x) \\
&\leq \beta + \phi_i''(\mu_{h_i}) + \frac{K_4}{2} \left[\phi_i''(\mu_0) + \beta - B \right]^{-1}
\end{aligned} \tag{25}$$

where we have used a Taylor expansion and the coarse-bound on $\text{var}_{h_i}(x)$ (eq. (19)).

This gives us an upper-bound on β_i :

$$\begin{aligned}
\beta_i &\leq \phi_i''(\mu_{h_i}) + \frac{K_4}{2} \left[\phi_i''(\mu_0) + \beta - B \right]^{-1} \\
&\leq \phi_i''(\mu_{h_i}) + \mathcal{O}(K_4 \beta^{-1})
\end{aligned} \tag{26}$$

Combining the upper and lower-bound (eqs. 24 and 26), we find that we can express the limit behavior of β_i as a function of μ_{h_i} :

$$\beta_i = \phi_i''(\mu_{h_i}) + \mathcal{O}(K_4 \beta^{-1} + K_3^2 \beta^{-2}) \tag{27}$$

This last result concludes our first section on $\text{var}_{h_i}(x)$ and β_i .⁵

Limit of μ_{h_i} The next step in our proof is to work on the mean of the hybrid. We will now show that $\mu_{h_i} \approx \mu_0$. This will give us the final expression: $\beta_i \approx \phi_i''(\mu_0)$ and will also be important in deriving the limit behavior of r_i .

We start from a ‘‘Stein relationship’’: with integration by parts, we find that it would be true that, for any probability distribution, the expected value of the log-gradient of the distribution is always equal to 0:

$$E_p \left(\psi'(x) \right) = 0 \tag{29}$$

where we have used $p(x) \propto \exp(-\psi(x))$ as an example.

We then apply that relationship to h_i whose log-gradient has contributions from the site and from the cavity distribution:

$$E_{h_i} \left(\phi_i'(x) + x\beta - (\beta\mu_0 - \delta r) \right) = 0 \tag{30}$$

$$\beta [\mu_{h_i} - \mu_0] = -\delta r - E_{h_i} \left(\phi_i'(x) \right) \tag{31}$$

We now perform a Taylor expansion of $E_{h_i} \left(\phi_i'(x) \right)$:

$$E_{h_i} \left(\phi_i'(x) \right) \approx \phi_i'(\mu_0) + \phi_i''(\mu_0) [\mu_{h_i} - \mu_0] \tag{32}$$

The error in that expression can be upper-bounded:

$$\begin{aligned}
\text{error} &\leq \frac{K_3}{2} \text{var}_{h_i}(x) \\
&\leq \frac{K_3}{2} \left[\phi_i''(\mu_0) + \beta - B \right]^{-1} \\
&\leq \mathcal{O}(K_3 \beta^{-1})
\end{aligned} \tag{33}$$

⁴Consider estimating x from the observation $\hat{x} = x + \eta$ where the noise has distribution $h_i(\eta - \mu_{h_i})$: it has mean 0 and variance var_{h_i} . \hat{x} is an unbiased estimator with variance var_{h_i} . The Fisher information in \hat{x} about x is: $E_{h_i} \left(\phi_i''(x) + \beta \right)$. This gives the claimed Cramer-Rao inequality.

See example 10.22 from Saumard et al (2014).

⁵Note also the slight variant:

$$\beta_i = E_{h_i} \left(\phi_i''(x) \right) + \mathcal{O}(K_3^2 \beta^{-2}) \tag{28}$$

This variant is not used again in the rest of the work we present here but is the next order of the expansion of β_i which could be of interest in expansions.

We combine that Taylor expansion (32) and that bound (33) with the Stein relationship (31):

$$\left[\beta + \phi_i''(\mu_0)\right] [\mu_{h_i} - \mu_0] = -\delta r - \phi_i'(\mu_0) + \mathcal{O}(K_3\beta^{-1}) \quad (34)$$

From which we can deduce a coarse bound on $\mu_{h_i} - \mu_0$:

$$\begin{aligned} \mu_{h_i} - \mu_0 &= \left[\beta + \phi_i''(\mu_0)\right]^{-1} \left[-\delta r - \phi_i'(\mu_0)\right] + \mathcal{O}(K_3\beta^{-2}) \\ &= \mathcal{O}\left(\left[\delta r + \phi_i'(\mu_0)\right] \beta^{-1} + K_3\beta^{-2}\right) \end{aligned} \quad (35)$$

This coarse bound will now be used to slightly update eq. (24) in order to remove the dependency on μ_{h_i} and obtain the final equation on the limit behavior of β_i . We will also use it in the final section to compute the limit behavior of r_i .

Returning to β_i We combine the coarse bound on μ_{h_i} with our expression for the limit behavior of β_i . We find:

$$\begin{aligned} \beta_i - \phi_i''(\mu_0) &= \phi_i''(\mu_{h_i}) - \phi_i''(\mu_0) + \mathcal{O}(K_4\beta^{-1} + K_3^2\beta^{-2}) \\ &= \mathcal{O}(K_3[\mu_{h_i} - \mu_0] + K_4\beta^{-1} + K_3^2\beta^{-2}) \\ &= \mathcal{O}\left(K_3\left[\delta r + \phi_i'(\mu_0)\right] \beta^{-1} + K_3^2\beta^{-2} + K_4\beta^{-1} + K_3^2\beta^{-2}\right) \end{aligned} \quad (36)$$

Which completely concludes the proof for the expression of the limit behavior of β_i .

Limit of $r_i = \text{var}_{h_i}^{-1}(x) \mu_{h_i} - (\beta\mu_0 - \delta r)$ We now turn to the task of approximating r_i . Our very first step here is to use the Stein relationship we already used above (eq. (30)). This gives a simple expression for r_i without going through the limit behavior of the hybrid mean and the hybrid variance.

We start from the Stein relationship we had before (eq. (30)):

$$\begin{aligned} E_{h_i}\left(\phi_i'(x) + x\beta - (\beta\mu_0 - \delta r)\right) &= 0 \\ E_{h_i}\left(\phi_i'(x)\right) + \beta\mu_{h_i} - \beta\mu_0 + \delta r &= 0 \end{aligned} \quad (37)$$

Let $g(x)$ be the Gaussian with same mean and variance as the hybrid. The natural parameters of g are the sum of the natural parameters of the cavity distribution and of the approximation of h_i . In other words, its natural parameters are $\beta + \beta_i$ and $\beta_i\mu_0 - \delta r + r_i$:

$$g = \mathcal{P}(h_i) \propto \exp\left(-[\beta + \beta_i] \frac{x^2}{2} + [\beta\mu_0 - \delta r + r_i] x\right)$$

If we now apply the Stein relationship to g , we find:

$$\begin{aligned} E_g([\beta + \beta_i] x - (\beta\mu_0 - \delta r + r_i)) &= 0 \\ (\beta_i\mu_{h_i} - r_i) + (\beta\mu_{h_i} - \beta\mu_0 + \delta r) &= 0 \end{aligned} \quad (38)$$

Combining these two equations (37), (38), we find:

$$r_i = \beta_i\mu_{h_i} - E_{h_i}\left(\phi_i'(x)\right) \quad (39)$$

which is a nice simple expression for r_i . We have thus found a way to work directly on r_i while avoiding direct work on the mean and variance.⁶

We will now simplify eq. (39). We start from a slight rewriting:

$$r_i = \beta_i\mu_0 + \beta_i(\mu_{h_i} - \mu_0) - E_{h_i}\left(\phi_i'(x)\right) \quad (40)$$

⁶Note that, in the exact same way as for eq. (28), this equation is interesting in its own right for expansions of our result as it is the next order of the expression for r_i .

Let's expand the $E_{h_i}(\phi'_i(x))$ term. We just perform a Taylor expansion (around μ_0):

$$\begin{aligned} E_{h_i}(\phi'_i(x)) &= \phi'_i(\mu_0) + \phi''_i(\mu_0)(\mu_{h_i} - \mu_0) + \mathcal{O}\left(K_3\left(\text{var}_{h_i} + (\mu_{h_i} - \mu_0)^2\right)\right) \\ &= \phi'_i(\mu_0) + \phi''_i(\mu_0)(\mu_{h_i} - \mu_0) + \mathcal{O}\left(K_3\beta^{-1} + K_3(\mu_{h_i} - \mu_0)^2\right) \end{aligned} \quad (41)$$

This gives us the following expression for r_i :

$$r_i \approx \beta_i\mu_0 - \phi'_i(\mu_0) + \left(\beta_i - \phi''_i(\mu_0)\right)(\mu_{h_i} - \mu_0) \quad (42)$$

We now just need to bound $\beta_i - \phi''_i(\mu_0)$ to finalize our proof, which we have already done in eq. (36). We then obtain the final expression for the limit behavior of r_i :

$$\begin{aligned} r_i - \beta_i\mu_0 - \phi'_i(\mu_0) &= \mathcal{O}\left(\left(\beta_i - \phi''_i(\mu_0)\right)(\mu_{h_i} - \mu_0) + K_3\beta^{-1} + K_3(\mu_{h_i} - \mu_0)^2\right) \\ &= \mathcal{O}\left(K_3\beta^{-1} + K_4\beta^{-1}(\mu_{h_i} - \mu_0) + K_3(\mu_{h_i} - \mu_0)^2\right) \end{aligned} \quad (43)$$

□

5.3 Limit behavior in high-dimensions

Our result generalizes to the p -dimensional case: when the probability distribution we are trying to approximate concerns a p -dimensional random variable.

The main difficulty in stating and in understanding that case comes from the tensor notation that we have to work with. Indeed, all of the moments and the derivatives we have to work with shift from being scalars to being p -dimensional tensors of various orders.

5.3.1 Tensor notation and rephrasing the assumptions

Let's first recall what tensors are. A tensor of order k is simply a multilinear mapping of $(\mathbb{R}^p)^k$ to \mathbb{R} : it takes k vectors and returns a scalar. We will note this $T[v_1, v_2 \dots v_k]$. This is a simple extension of vectors (order 1 tensors) and matrices (order 2 tensors). In our examples, we will always deal with symmetric tensors for which the order of the arguments does not influence the outputted value. Finally, an order k tensor can be also be used as a multilinear mapping with fewer than $l < k$ entries: it then returns an order $k - l$ tensor. This simply corresponds to specifying some of the inputs to the original tensor and leaving the assignation of the other inputs for latter. We will note by leaving to be specified inputs with a minus sign: eg $T[v_1 \dots v_{k-2}, -, -]$ for $l = 2$. For example, if we were to perform a Taylor expansion of $\nabla\phi(\mathbf{x})$, this Taylor expansion would need to return a vector (ie: an order 1 tensor). The first term of the expansion would be $H\phi_i(\mathbf{x}_0)[(\mathbf{x} - \mathbf{x}_0), -]$, the second term $\phi_i^{(3)}[(\mathbf{x} - \mathbf{x}_0), (\mathbf{x} - \mathbf{x}_0), -]$, etc.

In order to state our result in p -dimensions, we will first need to extend our assumptions to the high-dimensional case. This is relatively easy for the boundedness condition on $H\phi_i$: we just need to find a matrix \mathbf{B} such that:

$$\forall \mathbf{x}_1, \mathbf{x}_2 \quad H\phi_i(\mathbf{x}_1) - H\phi_i(\mathbf{x}_2) \leq \mathbf{B} \quad (44)$$

where the order relationship is the standard (semi) order between symmetric matrices: $\mathbf{B}_1 \geq \mathbf{B}_2$ if their difference is positive semi-definite. This captures the idea that the range of the second derivatives is small.

The boundedness condition on the higher-derivatives requires us to define a norm on tensors. We will simply use the norm induced on tensors by the L_2 norm on vectors. This is defined, for a tensor of order k by:

$$\|T\| = \max_{v_1 \dots v_k} \frac{T[v_1 \dots v_k]}{\prod \|v_i\|_2} \quad (45)$$

For vectors (who are order 1 tensors), this is of course the L_2 norm. For matrices, this corresponds to the maximum eigenvalue.

This induced norm has good behavior when we input an order k tensor T_k with only l inputs: the resulting order $k - l$ tensor $T_{k-l} = T_k [v_1 \dots v_l, -, \dots, -]$ has bounded norm:

$$\|T_{k-l}\| \leq \|T_k\| \prod_{i=1}^l \|v_i\|_2 \quad (46)$$

This simply follows from the definition of the norm. We will use this fact several times because we often need to perform Taylor expansion of gradient vectors or of Hessian matrices. For example, if we perform an order 0 Taylor expansion of $H\phi_i(\mathbf{x})$ around $\boldsymbol{\mu}_0$, we can use this result to bound the matrix-valued reminder term:

$$\begin{aligned} R_3(\mathbf{x}) &= H\phi_i(\mathbf{x}) - H\phi_i(\boldsymbol{\mu}_0) \\ \|R_3(\mathbf{x})\| &\leq K_3 \|\mathbf{x} - \boldsymbol{\mu}_0\| \end{aligned}$$

Once we have defined this norm, we can define the infinity norm for a tensor-valued function like the third derivative and the fourth derivative. We can then state our second assumption in p -dimensions:

$$\left\| \phi_i^{(3)} \right\|_{\infty} \leq K_3 \quad (47)$$

$$\left\| \phi_i^{(4)} \right\|_{\infty} \leq K_4 \quad (48)$$

5.3.2 Updating the proof

Let's now see how our proof changes now that we are in the high-dimensional case.

Summary of the differences All the important steps of the proof are identical: the Brascamp-Lieb theorem, the Cramer-Rao bound, the Stein's method trick all work in high-dimensions. Thus, the algebra of the proof is the same. What does change is the bounding of the error terms: throughout the proof, we repeatedly bound $E_{h_i} \left((x - \mu_{h_i})^2 \right)$ which corresponds in high-dimensions to $E_{h_i} \left(\|\mathbf{x} - \boldsymbol{\mu}_{h_i}\|^2 \right)$. In 1D, we bounded this using the coarse bound on the variance of the hybrid we got from the Brascamp-Lieb theorem:

$$\text{var}_{h_i}(x) \leq [H\phi_i(\boldsymbol{\mu}_0) + \beta - B]^{-1}$$

We will do the exact same thing in high-dimensions. Let's note \mathbf{Q} the precision matrix of the cavity distribution. The coarse variance bound reads:

$$\text{Cov}_{h_i}(\mathbf{x}) \leq [H\phi_i(\boldsymbol{\mu}_0) + \mathbf{Q} - \mathbf{B}]^{-1}$$

which gives:

$$\begin{aligned} E_{h_i} \left(\|\mathbf{x} - \boldsymbol{\mu}_{h_i}\|^2 \right) &\leq \text{Tr} \left([H\phi_i(\boldsymbol{\mu}_0) + \mathbf{Q} - \mathbf{B}]^{-1} \right) \\ &\leq p \left\| [H\phi_i(\boldsymbol{\mu}_0) + \mathbf{Q} - \mathbf{B}]^{-1} \right\| \end{aligned}$$

which gives us the effect of the dimension parameter p on our results: it scales the error (at most) linearly.

An example: going through the bound on \mathbf{Q}_i Now that we have given a high-level explanation of the difference between the two cases, let's detail how the proof of the result needs to be extended for the bound on \mathbf{Q}_i .

In the 1D proof, we bounded: $\text{var}_{h_i}(H\phi_i(x))$ using a Taylor expansion. In high-dimensions, this gives:

$$\begin{aligned} \|H\phi_i(\mathbf{x}) - H\phi_i(\boldsymbol{\mu}_{h_i})\| &\leq K_3 \|\mathbf{x} - \boldsymbol{\mu}_{h_i}\| \\ \|H\phi_i(\mathbf{x}) - H\phi_i(\boldsymbol{\mu}_{h_i})\|^2 &\leq K_3^2 \|\mathbf{x} - \boldsymbol{\mu}_{h_i}\|^2 \end{aligned}$$

We then have:

$$\begin{aligned}
\text{var}_{h_i}(H\phi_i(x)) &\leq K_3^2 E_{h_i}(\|\mathbf{x} - \boldsymbol{\mu}_{h_i}\|^2) \\
&\leq K_3^2 \text{Tr}(\text{Cov}_{h_i}(\mathbf{x})) \\
&\leq K_3^2 \text{Tr}([H\phi_i(\boldsymbol{\mu}_0) + \mathbf{Q} - \mathbf{B}]^{-1}) \\
&\leq pK_3^2 \|[H\phi_i(\boldsymbol{\mu}_0) + \mathbf{Q} - \mathbf{B}]^{-1}\|
\end{aligned}$$

where we have used the coarse bound on the covariance of the hybrid distribution that we obtained from the Brascamp-Lieb theorem.

The high-dimensional theorem This then leads us to the following theorem stating our limit result in high-dimensions. Note that the ‘‘high precision’’ limit here means that *all* eigenvalues of \mathbf{Q} should go to infinity.

Theorem 6. *High-dimensional extension*

Th. 5 also applies when approximating a target distribution over a p -dimensional space. The small term is then

$$\epsilon = \max(K_3, K_4) \text{Tr}([H\phi_i(\boldsymbol{\mu}_0) + \mathbf{Q} - \mathbf{B}]^{-1}) \quad (49)$$

$$\leq p \max(K_3, K_4) \|[H\phi_i(\boldsymbol{\mu}_0) + \mathbf{Q} - \mathbf{B}]^{-1}\| \quad (50)$$

Remark. In this result, the error scales linearly with the dimensionality of the space over which the target distribution is expressed. This means that, in the non-parametric case for which $p = n$, our results stop providing useful bounds, and it wouldn’t be possible to prove that EP is asymptotically exact. We believe that this is a weakness of our proof and not of EP, and that a more careful bounding of the error would show that EP still behaves properly in non-parametric problems.

5.4 Limit behavior under weaker assumptions

Our choice of constraints in the main text is restrictive: while it can be applied for wide classes of statistical models, it’s still quite far from being a necessary condition. In this section, we expose an alternative set of assumptions such that a variant of theorem 5 holds.

In this section, we will simply use a global bounding of the site:

$$l_i(x) \leq 1 \quad (51)$$

We will also replace our global assumption constraining the higher log-derivatives of the sites with a purely local constraint: we assume that there exists a compact neighborhood \mathcal{I} of μ_0 such that ϕ_i is derivable four times, and that those four derivatives are bounded inside \mathcal{I} .

Theorem 7. *Global bounding of the site (eq. 51) and local smoothness constraints are sufficient for th. 5 to hold*

Proof. The key idea behind this proof is the following: we will show that under our assumptions the sequence of probability densities $h_i(x|\beta)$ converges towards their restrictions to \mathcal{I} . This convergence is strong enough to imply convergence of the parameters of the Gaussian approximation. Since the restriction of the site to \mathcal{I} : $l_i(x) 1(x \in \mathcal{I})$ fulfills the hypotheses of the weaker theorem, we get the claimed result.

Convergence of $h_i(x|\beta)$ As a first step, let’s slightly rewrite the ‘‘cavity’’ Gaussian by centering it around its limit mean μ_0 :

$$\begin{aligned}
q_{-i} &\propto \exp\left(-\frac{\beta}{2}x^2 + (\beta\mu_0 - \delta r)x\right) \\
&\propto \exp\left(-\frac{\beta}{2}(x - \mu_0)^2 - \delta r(x - \mu_0)\right)
\end{aligned}$$

Now consider the sequence of probability density functions:

$h_i(x|\beta) = \frac{l_i(x)}{l_i(\mu_0)} \sqrt{\frac{\beta}{2\pi}} \exp\left(-\frac{\beta}{2}(x - \mu_0)^2 - \delta r(x - \mu_0)\right)$. Note that these are unproperly normalized. However, in the limit, the sequence of integrals $\int h_i(x|\beta) \rightarrow 1$ as we will now show.

Note $M_\beta(t) = \int \exp(t\sqrt{\beta}(x - \mu_0)) h_i(x|\beta) dx$: this is the moment generating function of the random variable $y_\beta = \sqrt{\beta}(x - \mu_0)$ (though, once again, note that this is only an asymptotically properly normalized density as our proof that $M_\beta(0) \rightarrow 1$ will show). For any $\beta > 0$, $M_\beta(t)$ is finite (the quadratic terms in the log dominate and $l_i(x) \leq 1$).

Let's prove that $M_\beta(t)$ converges pointwise for any value of t to $\exp\left(-\frac{t^2}{2}\right)$. This will prove that y_β converges to a Gaussian of variance 1, and that its density is asymptotically properly normalized.

Fix t . Let $\epsilon > 0$. Since the derivatives are bounded on \mathcal{I} , there must exist a ball centered on $\mu_0 : B(\mu_0, r_\epsilon) \subset \mathcal{I}$, where $|l_i(x) - l_i(\mu_0)| \leq \epsilon$. Let's decompose the integral in M_β into the integral over B (where that simple bound holds) and the one over \mathbb{R}/B .

For the central region:

$$\begin{aligned} \text{cent}(\beta) &= \int_B \exp\left(\sqrt{\beta}t(x - \mu_0)\right) h_i(x|\beta) \\ &\geq \frac{l_i(\mu_0) - \epsilon}{l_i(\mu_0)} \sqrt{\frac{\beta}{2\pi}} \int_B \exp\left(\sqrt{\beta}t(x - \mu_0) - \frac{\beta}{2}(x - \mu_0)^2 - \delta r(x - \mu_0)\right) \\ &\geq \frac{l_i(\mu_0) - \epsilon}{l_i(\mu_0)} \sqrt{\frac{\beta}{2\pi}} \int_B \exp\left(\frac{\beta}{2}\left(x - \mu_0 - \frac{t}{\sqrt{\beta}}\right)^2 + \frac{(t - \delta r/\sqrt{\beta})^2}{2}\right) \end{aligned}$$

and a similar upper-bound.

As $\beta \rightarrow \infty$, all of the mass of $\sqrt{\beta} \exp\left(\frac{\beta}{2}\left(x - \mu_0 - \frac{t}{\sqrt{\beta}}\right)^2\right)$ becomes concentrated inside B . Thus, the bounds converge to $\frac{l_i(\mu_0) \pm \epsilon}{l_i(\mu_0)} \exp\left(\frac{t^2}{2}\right)$ as $\beta \rightarrow \infty$.

For the exterior region:

$$\begin{aligned} \text{ext}(\beta) &= \int_{x \notin B} \exp\left(\sqrt{\beta}t(x - \mu_0)\right) h_i(x|\beta) \\ &\leq \frac{\sqrt{\beta}}{l_i(\mu_0)} \int_{x \notin B} \exp\left(\sqrt{\beta}t(x - \mu_0) - \frac{\beta}{2}(x - \mu_0)^2 - \delta r(x - \mu_0)\right) \\ &\leq \frac{\sqrt{\beta}}{l_i(\mu_0)} \int_{x \notin B} \exp\left(\frac{\beta}{2}\left(x - \mu_0 - \frac{t}{\sqrt{\beta}}\right)^2 + \frac{(t - \delta r/\sqrt{\beta})^2}{2}\right) \end{aligned}$$

which converges to 0 as $\beta \rightarrow \infty$ (exponentially fast), since all of the probability mass of $\sqrt{\beta} \exp\left(\frac{\beta}{2}\left(x - \mu_0 - \frac{t}{\sqrt{\beta}}\right)^2\right)$ is concentrated inside B .

With those convergences, we could thus find β_0 such that $\forall \beta \geq \beta_0$,

$$\left| M_\beta(t) - \exp\left(-\frac{t^2}{2}\right) \right| \leq 3\epsilon \exp\left(\frac{t^2}{2}\right) (l_i(\mu_0))^{-1} \quad (52)$$

This proves that $M_\beta(t)$ converges pointwise to $\exp\left(-\frac{t^2}{2}\right)$.

$M_\beta(t)$ is the moment generating function of an unnormalized probability distribution. The moment generating function for the normalized variable is simply found by taking the ratio against $M_\beta(0)$. Since $M_\beta(0)$, the MGF of the normalized density also converges to $\exp\left(-\frac{t^2}{2}\right)$:

$$\lim_{\beta \rightarrow \infty} \frac{M_\beta(t)}{M_\beta(0)} \rightarrow \exp\left(-\frac{t^2}{2}\right)$$

Note that this means that the sequence of random variables y_β converges in MGF to a Gaussian centered at 0 and with variance 1. Convergence in MGF implies weak-convergence and convergence of all moments, and implies the convergence of x_β to a Gaussian centered at μ_0 and with variance β^{-1} . However, this is a secondary point: we will have to work directly on $M_\beta(t)$ in order to derive our next results.

Convergence of $h_i(x|\beta)$ to its restriction to \mathcal{I} We will use this MGF convergence to prove that $h_i(x|\beta)$ converges to its restriction to \mathcal{I} : $h_i^r(x|\beta) = h_i(x|\beta) 1(x \in \mathcal{I})$, and furthermore that the error we make in this approximation are negligible compared to the limit behavior of interest in μ_{h_i} and in var_{h_i} .

Let's first prove the convergence of the variances. h_i^r fulfills the hypotheses of the less-general theorem 5, so that:

$$\text{var}_{h_i^r}(x) \approx \beta^{-1} + \beta^{-2} \phi_i''(\mu_0) + \mathcal{O}(\beta^{-3})$$

The important feature is that the deviation of interest from the β^{-1} limit is of order β^{-2} .

Let's compute the variance for the unrestricted hybrid h_i . We can decompose the variance into the contribution from \mathcal{I} and the contribution from $\mathbb{R} \setminus \mathcal{I}$. The contribution from the outer region can be upper-bounded by the following argument:

- Let t_0 such that $\exp(-|t_0(x - \mu_0)|)(x - \mu_0)^2$ is strictly decreasing on the outer region $\mathbb{R} \setminus \mathcal{I}$.
- Let's recall the Markov-bound: it proves that a positive random-variable with finite mean can not have arbitrarily large deviations. It can be extended to prove that a positive random-variable with finite k^{th} moment must also have bounded k_2^{th} moments for all $k_2 < k$.

Because $\exp(-|t_0(x - \mu_0)|)(x - \mu_0)^2$ is decreasing, we can find a Markov-like bound on the contribution of the outer region of h_i to the variance. Note ρ the radius of \mathcal{I} and consider the following bound on $(x - \mu_0)^2 1(x \notin \mathcal{I})$:

$$\begin{aligned} \exp(-|t_0(x - \mu_0)|)(x - \mu_0)^2 1(x \notin \mathcal{I}) &\leq \exp(-|t_0\rho) \rho^2 \\ (x - \mu_0)^2 1(x \notin \mathcal{I}) &\leq \exp(|t_0(x - \mu_0)|) \exp(-|t_0\rho) \rho^2 \end{aligned}$$

When we take the expected value under h_i , we obtain the Markov-like bound:

$$\begin{aligned} E_{h_i} \left((x - \mu_0)^2 1(x \notin \mathcal{I}) \right) &\leq E_{h_i} \left(\exp(|t_0(x - \mu_0)|) \exp(-|t_0\rho) \rho^2 \right) \\ &\leq \frac{1}{M_\beta(0)} \left(M_\beta \left(-\frac{t_0}{\sqrt{\beta}} \right) + M_\beta \left(\frac{t_0}{\sqrt{\beta}} \right) \right) \exp(-|t_0\rho) \rho^2 \end{aligned}$$

- Now consider adapting that last bound to the value of β with $t_\beta = \sqrt{\beta}t_0$ (note that for $t \geq t_0$, the corresponding function is still decreasing outside of \mathcal{I}). We get:

$$E_{h_i} \left((x - \mu_0)^2 1(x \notin \mathcal{I}) \right) \leq \frac{1}{M_\beta(0)} (M_\beta(-t_0) + M_\beta(t_0)) \exp\left(-\left|\sqrt{\beta}t_0\rho\right|\right) \rho^2$$

and since the $M_\beta(\pm t_0)$ converge to $\exp\left(\frac{t_0^2}{2}\right)$, we have that, for sufficiently high β :

$$E_{h_i} \left((x - \mu_0)^2 1(x \notin \mathcal{I}) \right) \leq \left(2 \exp\left(\frac{t_0^2}{2}\right) + \epsilon \right) \exp\left(-\left|\sqrt{\beta}t_0\rho\right|\right) \rho^2$$

This proves that the contribution of the outer region to the variance decreases exponentially in $\sqrt{\beta}$ which is much faster than the error in the central region which is in β^{-2} .

The error in the central region is thus found to dominate the other error terms so that $\text{var}_{h_i}^{-1} - \beta \rightarrow \text{var}_{h_i^r}^{-1} - \beta$.

By a similar argument, we can prove that the deviation of the mean from μ_0 is also dominated by the error in the central region, and that the error contributed by the outer region decays exponentially. This is done by finding t_0 such that $\exp(-|t_0(x - \mu_0)|)|x - \mu_0|$. This proves that: $\text{var}_{h_i}^{-1} E_{h_i}(x) - \beta\mu_0 \rightarrow \text{var}_{h_i^r}^{-1} E_{h_i^r}(x) - \beta\mu_0$ exponentially fast, while the size of the central term is of order 1.

We thus have that the Gaussian approximations of the $h_i(x|\beta)$ converges towards the Gaussian approximations of $h_i^r(x|\beta)$. Since we can apply the weaker theorem to $h_i^r(x|\beta)$, we get the claimed result. \square

5.5 Detailed proof of the stable region theorem

In this section, we detail the proof of the main text theorem on stable regions of aEP and EP.

Theorem 8. *Convergence of fixed points of EP and aEP*

There exists an EP and an aEP fixed point close to the CGA of $p(x)$ at x^* if $\phi_i''(x^*)$ is sufficiently large. More precisely, if:

$$\begin{aligned}\delta_{aEP} &= \max(K_3, K_4) \sum \left| \phi_i'(x^*) \right| \left[\psi''(x^*) \right]^{-1} \\ \delta &= n \max(K_3, K_4) \left[\psi''(x^*) \right]^{-1}\end{aligned}$$

are order 1 quantities and $\psi''(x^*)$ is large, then the limit of the stable regions on the global approximation, $n\Delta_r$ and $n\Delta_\beta$, scale as $\mathcal{O}(\delta_{aEP} + \delta)$ for aEP and as $\mathcal{O}(\delta)$ for EP.

Proof. Let's start with aEP. Let's assume that we start from region of the parameter space with the following form:

$$\begin{aligned}|r_{aEP} - \beta_{aEP}x^*| &\leq \gamma(\delta + \delta_{aEP}) \\ |\beta_{aEP} - \psi''(x^*)| &\leq \gamma(\delta + \delta_{aEP})\end{aligned}$$

The critical feature here is that the stable region has size of order 1 and that $\psi''(x^*)$ is large.

We will now apply th. 5 with $\mu_0 = x^*$ to bound the next parameter values:

$$\begin{aligned}r_{aEP}^{new} &= \beta_{aEP}^{new}x^* + \mathcal{O}\left(n \max(K_3, K_4) \left[\psi''(x^*) \right]^{-1}\right) \\ \beta_{aEP}^{new} &= \psi''(x^*) + \mathcal{O}\left(n \max(K_3, K_4) \left[\psi''(x^*) \right]^{-1}\right) \\ &\quad + \mathcal{O}\left(\max(K_3, K_4) \left[|r_{aEP} - \beta_{aEP}x^*| + \sum_{i=1}^n \left| \phi_i'(x^*) \right| \right] \left[\psi''(x^*) \right]^{-1}\right)\end{aligned}\tag{53}$$

In those equations, we have used the fact that $\mathcal{O}\left(\left[\frac{n-1}{n}\psi''(x^*) - |\beta_{aEP} - \psi''(x^*)|\right]^{-1}\right) = \mathcal{O}\left(\left[\psi''(x^*)\right]^{-1}\right)$. Note how the order 1 deviation: $|\beta_{aEP} - \psi''(x^*)|$ does not affect the limit behavior.

Similarly, the order 1 deviation in r : $|r_{aEP} - \beta_{aEP}x^*|$, is similarly ‘‘asymptotically silent’’: $|r_{aEP} - \beta_{aEP}x^*| \left[\psi''(x^*) \right]^{-1}$ is negligible before $\sum_{i=1}^n \left| \phi_i'(x^*) \right| \left[\psi''(x^*) \right]^{-1}$.

The limit behavior thus simplifies into:

$$\begin{aligned}r_{aEP} &= \beta_{aEP}x^* + \mathcal{O}(\delta) \\ \beta_{aEP} &= \psi''(x^*) + \mathcal{O}(\delta + \delta_{aEP})\end{aligned}$$

When $\psi''(x^*)$ is sufficiently large, there exists c such that: $|r_{aEP} - \beta_{aEP}x^*| \leq c\delta$. If $\gamma \geq c$, then this proves that the aEP iteration is contractive for the linear-shift natural parameter.

Similarly, when $\psi''(x^*)$ is sufficiently large, $|\beta_{aEP} - \psi''(x^*)| \leq c_2(\delta + \delta_{aEP})$, and if $\gamma \geq \max(c, c_2)$, the aEP iteration is contractive in both directions which proves the result.

The result for EP follows from the exact same reasoning. \square

5.6 Exactness of aEP and EP in the large-data limit

In this final section, we will prove our only non-deterministic result concerning the behavior of EP and aEP. We will prove that, if we accumulate sites which are generated according to some process guaranteeing Local Asymptotic Normality of the log-posterior, then aEP and EP have a fixed point which converges to the CGA in total-variation. Furthermore, if the process generating the sites respects some assumptions which constrain the mass of the posterior outside of a

close neighborhood of the highest-mode, then the posterior $p_n(x)$ and its CGA $q_n(x)$ converge towards one another in total-variation. This ensures that aEP and EP both have a fixed point which is asymptotically exact in total-variation.

We were unable to obtain a Bernstein-von Mises results which offers exactly the conditions we needed, so we we had to re-derive every result from scratch. We make no claim for originality for this section which is extremely similar to many other asymptotic studies of likelihoods and posterior distributions.

Let's first detail the assumptions that we will need on the random process generating the sites $l_i(x)$. We will assume that:

- the l_i are i.i.d
- Their distribution is such that the expected value function:

$$x \rightarrow E(\phi_i(x))$$

has a global maximum at x_0 . We will note $I_0 = E(\phi_i''(x_0)) > 0$.

- their distribution is such that the following quantities are finite:

$$\begin{aligned} \text{var}(\phi_i''(x_0)) &< \infty \\ \text{var}(\phi_i'(x_0)) &< \infty \\ E(|\phi_i'(x_0)|) &< \infty \end{aligned}$$

Their size controls how regular the process generating the sites is. Note that, in the well-specified case, $\text{var}(\phi_i'(x_0)) = E(\phi_i''(x_0)) = I_0$ by integration by parts, in which case I_0 is the Fisher information provided by the observations.

These conditions will ensure that the posterior is Locally Asymptotically Normal so that it can be approximated locally by a Gaussian. Furthermore, in order to have a global approximation, we will require that the model is such that estimation with it is consistent: with probability tending to 1, it converges towards x_0 which is the parameter that fits the data best. The condition is that: $\forall \epsilon > 0$, the random variables $\int p_n(x) 1(|x - x_0| \leq \epsilon) dx$ converge to 1 in probability as $n \rightarrow \infty$. Armed with these assumptions, let's now derive several results on the log-posterior.

Lemma 9. *As $n \rightarrow \infty$, the log-curvature at x_0 grows linearly. More precisely, $\forall \epsilon > 0$:*

$$\sum_{i=1}^n \phi_i''(x_0) \geq n(I_0 - \epsilon)$$

with probability tending to 1. Similarly, the log-gradient at x_0 is of order \sqrt{n} . With probability tending to 1, we have that:

$$\left| \sum_{i=1}^n \phi_i'(x_0) \right| \leq \sqrt{n [\text{var}(\phi_i'(x_0)) + \epsilon]}$$

Proof. This result is simply a large-data limit concentration result.

The mean of the cumulative sum is nI_0 while its variance is $n \text{var}(\phi_i''(x_0))$. By Chebyshev's concentration theorem, the probability that the cumulative sum deviates from its mean decays at speed \sqrt{n} .

By the exact same argument, we get that the cumulative log-gradient is small: its mean is 0, by definition of x_0 , and its variance is $n \text{var}(\phi_i'(x_0))$. Once again, by applying Chebyshev's theorem, we get the claimed result. \square

Lemma 10. *As $n \rightarrow \infty$, there exists with probability tending to 1 a mode x_n^* in close proximity to x_0 . More precisely:*

$$x_0 - x_n^* = \mathcal{O}(n^{-1/2})$$

Throughout the following lemmas, we will always refer to x_n^* without explicitly mentioning that x_n^* does not always exist (but has probability tending to 1 of existing).

Proof. With lemma 9, we have that with probability 1, the log-curvature at x_0 grows linearly and the log-gradient is of order \sqrt{n} . Assume for the following that the log-gradient at x_0 is negative.

We also have that the third log-derivative is bounded:

$$\left| \sum_{i=1}^n \phi_i^{(3)}(x) \right| \leq nK_3$$

Let's then consider the following Taylor lower-bound to the log-gradient:

$$\sum_{i=1}^n \phi_i'(x) = \sum_{i=1}^n \phi_i'(x_0) + (x - x_0) \left(\sum_{i=1}^n \phi_i''(x) \right) - \frac{(x - x_0)^2}{2} nK_3$$

If the log-curvature is sufficiently large, and the log-gradient sufficiently small, the second degree polynomial in x has two roots. More precisely, this happens when the discriminant is positive:

$$Disc = \left(\sum_{i=1}^n \phi_i''(x) \right)^2 - 4 \left| \sum_{i=1}^n \phi_i'(x_0) \right| nK_3$$

Given the growth rates of the log-gradient and of the log-curvature, we have that, with probability 1, this discriminant is positive, because it grows asymptotically as \sqrt{n} . Thus, in the large-data limit, we are guaranteed to have a root in close vicinity of x_0 . Furthermore, it is easy to check that the dominating term in x_n^* is the root of the order 1 polynomial $\sum_{i=1}^n \phi_i'(x_0) + (x - x_0) \left(\sum_{i=1}^n \phi_i''(x) \right) = 0$:

$$x_n^* - x_0 = - \left(\sum_{i=1}^n \phi_i''(x) \right)^{-1} \left(\sum_{i=1}^n \phi_i'(x_0) \right) + \mathcal{O}(n^{-1})$$

This leading term is of order $n^{-1/2}$ which concludes this proof⁷. □

Lemma 11. *The log-curvature at x_n^* grows linearly with probability tending to 1. More precisely, $\forall \epsilon > 0$:*

$$\sum_{i=1}^n \phi_i''(x_n^*) \geq n(I_0 - \epsilon)$$

with probability tending to 1.

Similarly, the following quantity grows linearly:

$$\sum_{i=1}^n \left| \phi_i'(x_n^*) \right| \approx nE \left(\left| \phi_i'(x_0) \right| \right)$$

Proof. We compute the log-curvature at x_n^* from the log-curvature at x_0 with a Taylor expansion:

$$\left| \sum_{i=1}^n \phi_i''(x_n^*) - \phi_i''(x_0) \right| \leq nK_3 |x_n^* - x_0|$$

Since $|x_n^* - x_0|$ is of order $n^{-1/2}$, we get that the error between the two is of order \sqrt{n} and that the log-curvature at x_n^* grows linearly.

Similarly:

$$\left| \sum_{i=1}^n \left| \phi_i'(x_n^*) \right| - \sum_{i=1}^n \left| \phi_i'(x_0) \right| \right| \leq \left(\sum_{i=1}^n \left| \phi_i''(x_0) \right| \right) |x_n^* - x_0|$$

and we have that this quantity also grows linearly. □

⁷This proof is straightforward to extend to the high-dimensional case. One simply needs to diagonalize the $\left(\sum_{i=1}^n \phi_i''(x) \right)$ matrix.

With this result, we reach a turning point in our proof. So far, we have proved that x_n^* exists and that various quantities measured at x_n^* grow linearly (with probability tending to 1). This proves that the log-posterior is Locally Asymptotically Normal (LAN) around x_n^* (with probability tending to 1).

We will now show that the LAN behavior of the posterior ensures that aEP and EP have a stable region in a small neighborhood around x_n^* and that all global approximations of $p_n(x)$ inside that stable region converge towards $q_n(x)$: the CGA of $p_n(x)$ at x_n^* .

Lemma 12. *We can apply main text th. 3 to x_n^* with probability tending to 1.*

Thus, there exists a stable region of order 0:

$$\begin{aligned} n\Delta_{n,r} &= \mathcal{O}(n^0) \\ n\Delta_{n,\beta} &= \mathcal{O}(n^0) \end{aligned}$$

around the CGA at x_n^ .*

Proof. The log-curvature at the mode x_n^* grows linearly in n and so does $n \max(K_3, K_4)$. Similarly, for aEP, $\sum_{i=1}^n |\phi'_i(x_n^*)|$ grows linearly. Application of the theorem then gives that there exists a stable region in the large-data limit. \square

Lemma 13. *All Gaussian approximations of $p_n(x)$ inside the stable region of lemma 12 converge in KL divergence to $q_n(x)$: the CGA centered at x_n^* . This convergence in KL divergence implies a convergence in total-variation.*

More precisely: $\forall r, \beta$ such that:

$$\begin{aligned} |r - \beta x_n^*| &\leq n\Delta_{n,r} \\ \left| \beta - \sum_{i=1}^n \phi''_i(x_n^*) \right| &\leq n\Delta_{n,\beta} \end{aligned}$$

then:

$$\begin{aligned} KL(\mathcal{N}(x|r, \beta), q_n(x)) &= \mathcal{O}(n^{-1}) \\ d_{TV}(\mathcal{N}(x|r, \beta), q_n(x)) &= \mathcal{O}(n^{-1/2}) \end{aligned}$$

Proof. The formula for the KL divergence between two Gaussian distributions (parameterized with mean and variance) $q_1 = \mathcal{N}(\mu_1, \beta_1^{-1})$ and $q_2 = \mathcal{N}(\mu_2, \beta_2^{-1})$ is the following:

$$\begin{aligned} 2KL(q_1, q_2) &= \beta_2 (\mu_1 - \mu_2)^2 + \frac{(\beta_2 - \beta_1)}{\beta_1} - \log(\beta_2/\beta_1) \\ &\approx \beta_2 (\mu_1 - \mu_2)^2 + \frac{(\beta_2 - \beta_1)^2}{2\beta_1^2} \end{aligned}$$

where the approximation is valid when $\frac{(\beta_2 - \beta_1)}{\beta_1} \approx 0$.⁸

⁸In the high-dimensional case, the KL divergence is:

$$2KL(q_1, q_2) = (\boldsymbol{\mu}_1 - \boldsymbol{\mu}_2) \mathbf{Q}_2 (\boldsymbol{\mu}_1 - \boldsymbol{\mu}_2) + Tr(\mathbf{Q}_2 \mathbf{Q}_1^{-1}) - d - \log\left(\frac{|\mathbf{Q}_2|}{|\mathbf{Q}_1|}\right)$$

If \mathbf{Q}_1 and \mathbf{Q}_2 are co-diagonal, the complicated term $Tr(\mathbf{Q}_2 \mathbf{Q}_1^{-1}) - d - \log\left(\frac{|\mathbf{Q}_2|}{|\mathbf{Q}_1|}\right)$ is, like the 1D case, almost quadratic. Even when they are not co-diagonal:

$$\log(|\mathbf{Q}_2 + \Delta|) \approx Tr\left(\mathbf{Q}_1^{-1} \Delta + \frac{1}{2} \mathbf{Q}_1^{-1} \Delta \mathbf{Q}_1^{-1}\right)$$

so that the quadratic approximation is still valid:

$$2KL(q_1, q_2) \approx (\boldsymbol{\mu}_1 - \boldsymbol{\mu}_2) \mathbf{Q}_2 (\boldsymbol{\mu}_1 - \boldsymbol{\mu}_2) + \frac{1}{2} Tr\left([\mathbf{Q}_2 - \mathbf{Q}_1]^2 \mathbf{Q}_1^{-2}\right)$$

When we apply this expression to our distributions of interest, we find the following upper-bound for the KL divergence between any Gaussian approximation in the stable region and the CGA at x_n^* (slightly abusively, we use the quadratic limit approximation of the β dependent term):

$$\begin{aligned} 2KL &\leq \left(\sum_{i=1}^n \phi_i''(x_n^*) \right) \left(\frac{n\Delta_{n,r}}{\sum_{i=1}^n \phi_i''(x_n^*) - n\Delta_{n,\beta}} \right)^2 + \frac{1}{2} \left(\frac{n\Delta_{n,\beta}}{\sum_{i=1}^n \phi_i''(x_n^*) - n\Delta_{n,\beta}} \right)^2 \\ 2KL &\leq \mathcal{O}(n^{-1} + n^{-2}) \\ 2KL &\leq \mathcal{O}(n^{-1}) \end{aligned}$$

We finally apply Pinsker's inequality, which relates the KL divergence to the total-variation metric: $KL \geq 2(d_{TV})^2$ and we get the claimed result. \square

Lemma 14. *Kleijn et al. (2012) If $p_n(x)$ is Locally Asymptotically Normal and its mass concentrates near x_n^* , then:*

$$d_{TV}(p_n(x), q_n(x)) = \mathcal{O}(n^{-1/2})$$

Proof. We just sketch the proof of Kleijn et al.

Fix $\epsilon > 0$. Under our assumption, with probability 1, the mass of $p_n(x)$ concentrates inside the ball $|x - x_0| \leq \epsilon$ as $n \rightarrow \infty$.

By a simple Taylor expansion inside the ball around x_n^* , we find that the CGA $q_n(x)$ is a good approximation of $p(x)$. Some care must be taken to ensure the rate of convergence holds. \square

With these last two lemmas 13 and 14, we conclude our proof of the theorem: under our conditions, all aEP and EP fixed points near the CGA at x_n^* converge in total-variation (with speed $\mathcal{O}(n^{-1/2})$) to the true posterior $p_n(x)$.

5.7 Exactness on probit and logit regression

Let's now show that both for probit and logit regression, EP is exact.

In both cases, the likelihoods $l_i(\mathbf{x})$ have the following simple form:

$$l_i(\mathbf{x}) = a(\mathbf{v}_i^t \mathbf{x})$$

where \mathbf{v}_i is the vector of predictors for the i^{th} datapoint and a is the link function (or activation function) of the model. Both for the probit and the logit case, a is a log-concave function with bounded derivatives of all orders. Thus, as long as the predictor vectors \mathbf{v}_i are guaranteed to be bounded, then the l_i are guaranteed to respect our assumptions on the derivatives (eqs. 16 and 17). Furthermore, the log-concavity of a makes it so that we can get rid of the identifiability assumption, as identifiability is implied by the other assumptions.

Lemma 15. *If the Fisher information matrix is strictly positive $\mathbf{I}_0 > 0$, then the posterior distribution is identifiable.*

Proof. the posterior distribution is a product of log-concave distributions. It is thus log-concave.

Furthermore, for the posterior, the log-curvature at x_n^* is growing linearly almost at speed \mathbf{I}_0 and the log third derivative is bounded by nK_3 .

The case with the larger tails that fits this picture is somewhat like the Huber log-likelihood (quadratic center with linear tails): it has a central curved region surrounded by linear tails. More precisely, the log-curvature of the posterior is larger than:

$$\sum_{i=1}^n \phi_i''(\mathbf{x}) \geq \max \left(\sum_{i=1}^n \phi_i''(\mathbf{x}_n^*) - nK_3 \|\mathbf{x} - \mathbf{x}_n^*\|, 0 \right) \quad (54)$$

We can integrate the limit behavior of the log-curvature in this expression yielding:

$$\sum_{i=1}^n \phi_i''(\mathbf{x}) \geq n \max(\mathbf{I}_0 - K_3 \|\mathbf{x} - \mathbf{x}_n^*\|, 0) \quad (55)$$

Critically, the log-curvature grows (approximately) linearly with n . If we simply integrate the above expression twice, this remains true for the negative log-posterior:

$$\sum_{i=1}^n (\phi_i(\mathbf{x}) - \phi_i(\mathbf{x}_n^*)) \propto n \quad (56)$$

In order to conclude, we will use a brand new result: theorem III.1 of Pereyra (2016). Pereyra shows that, for a log-concave probability distribution, most of the mass is concentrated in a region where the negative log-posterior is not too high above the minimum. Eq. 56 shows that the negative log-posterior grows linearly with the number of data-points n . By applying Pereyra’s theorem, we have that the probability concentrates around \mathbf{x}_n^* which concludes our proof. \square

A probit or logit regression thus respects all of our hypotheses. Thus, in the large-data limit, both aEP and EP are exact on a probit or logit model, as long as the Fisher information matrix is strictly positive.

6 aEP: an alternative to EP ?

In the main text, we used aEP as a theoretical tool to study the asymptotics of EP, but could it hold practical interest as well? aEP is simpler than standard EP, and in particular it requires fewer matrix factorizations. In standard EP computing the covariance matrix of cavity distributions is a $\mathcal{O}(nm^3)$ or $\mathcal{O}(nm^2)$ operation (where m is the number of parameters), depending on the problem and the implementation. In aEP the covariance of the cavity is just $\frac{n}{n-1}\Sigma$, the current covariance matrix, so that forming the cavity distribution is a very cheap $\mathcal{O}(m^2)$ operation. Depending on m aEP may be substantially faster.

Another advantage of aEP is that, due to its much smaller parameter set ($\mathcal{O}(m^2)$ vs $\mathcal{O}(nm^2)$), generic numerical tools for fixed point iterations may be used out-of-the-box. We experimented with R package SQUAREM (Varadhan and Roland, 2008), a set of algorithms that seek to accelerate fixed point iterations. Our limited experimentation indicates that although SQUAREM does not always achieve speed-ups, the fact that step sizes are chosen makes aEP very robust.

On the other hand, since aEP is an asymptotic approximation of EP, we will incur a loss in performance. We ran some simulations to see how different aEP and EP are in practical examples. We picked two statistical models, Cauchy regression and probit regression. Probit regression is a well-know EP success story (Kuss and Rasmussen, 2005; Nickisch and Rasmussen, 2008), with well-behaved, log-concave sites. Cauchy regression features non-log concave sites and posterior distributions may be multimodal.

Probit regression is the following model:

$$\begin{aligned} y_i &= \text{sign}(\mathbf{x}_i^t \boldsymbol{\alpha} + \epsilon) \\ \epsilon &\sim \mathcal{N}(0, 1) \end{aligned}$$

where \mathbf{x}_i is a vector of covariates, while Cauchy regression is:

$$\begin{aligned} y_i &= \mathbf{x}_i^t \boldsymbol{\alpha} + \epsilon \\ \epsilon &\sim \text{Cauchy}(0, 1) \end{aligned}$$

in both cases inference is for the regression coefficients $\boldsymbol{\alpha}$. We used the standard factorization of the posterior (over likelihood sites) with hybrid moments computed numerically. The prior over $\boldsymbol{\alpha}$ was set in both cases to $\boldsymbol{\alpha} \sim \mathcal{N}(0, 1)$. The regressors $\mathbf{x}_i \in \mathbb{R}^4$ were B-spline functions evaluated on a grid of n locations over the unit interval. Data were generated according to the model. We ran aEP and EP for 20 passes at speed $\gamma = 0.4$, since the Cauchy likelihood induced occasional convergence problems.

To measure the difference between aEP and EP, we used a relative difference in means:

$$d_\mu = \frac{|\mu_{EP} - \mu_{aEP}|}{\min(\sigma_{EP}, \sigma_{aEP})} \quad (57)$$

which expresses how different the estimates are in units of standard deviations. Differences in estimated posterior variance was summarized by a ratio:

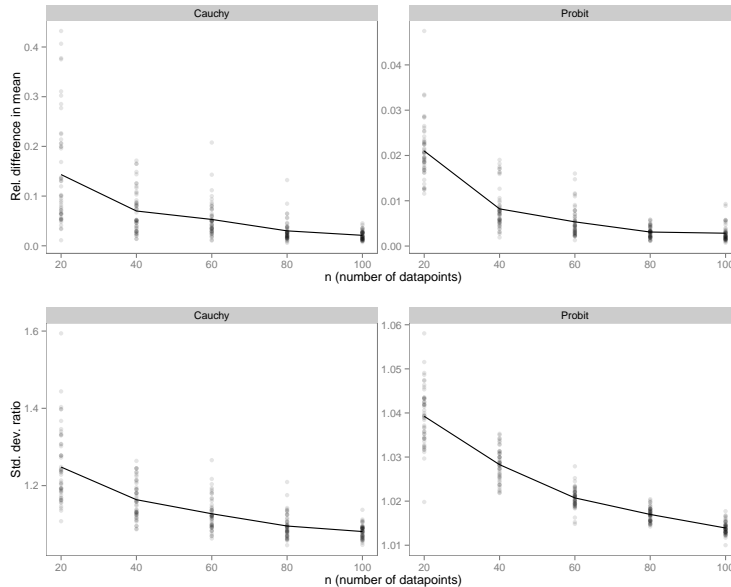


Figure 4: aEP vs EP in probit and Cauchy models. Note that the vertical scales are not the same across panels. Upper row: relative difference in means (eq. (57)) between aEP and EP. Lower row: ratio of standard deviations between aEP and EP (d_σ in (58)). Dots represent individual simulations, the continuous line connects the means.

$$d_\sigma = \max\left(\frac{\sigma_{EP}}{\sigma_{aEP}}, \frac{\sigma_{aEP}}{\sigma_{EP}}\right) \quad (58)$$

Both measures were averaged over the $m = 4$ parameters.

The results are shown on fig. 4. aEP and EP are both exact in large n , but the differences between the Cauchy and the probit model are notable (one order of magnitude). In the probit model aEP and EP are practically the same with just 20 datapoints, with relative differences in means reaching a maximum of 5%, whereas differences in the Cauchy model can reach 40%. With enough datapoints the differences disappear in the Cauchy model as well.

When applying aEP, one must be careful to remember that it uses the approximation that $\forall i, \lambda_i \approx \frac{1}{N} \sum \lambda_j$. This means that if a few sites are outliers and have a very exceptional contribution to the posterior, then they might make this approximation wrong and aEP might give a very poor approximation. If applying aEP, it thus seems sensible to check the validity of the assumption at the last point of the iteration as a simple sanity check to verify the quality of the approximation.

One interesting possibility is to run aEP until it gets close to a fixed point to take advantage of the smaller amounts of computations, and then switch to the EP iteration to take advantage of the possible increased precision of the EP algorithm.